2002

On the design of gain-scheduled trajectory tracking controllers

Silvestre, Carlos

C. Silvestre, A. Pascoal, and I. Kaminer, "On the design of gain-scheduled trajectory tracking controllers, "International Journal of Robust and Nonlinear Control, special issue on Gain-Scheduling, 2002, 12:797-839.

INTERNATIONAL JOURNAL OF ROBUST AND NONLINEAR CONTROL
Int. J. Robust Nonlinear Control 2002; **12**:797–839 (DOI: 10.1002/rnc.705)

On the design of gain-scheduled trajectory tracking controllers

Carlos Silvestre[1,*,†], Antonio Pascoal[1,‡] and Isaac Kaminer[2,§]

[1] *Department of Electrical Engineering and Computer Science and Institute for Systems and Robotics (ISR), Instituto Superior Tecnico, Av. Rovisco Pais, 1049-001 Lisbon, Portugal*
[2] *Department of Aeronautical and Astronautical Engineering, Naval Postgraduate School, Monterey, CA 93943, USA*

SUMMARY

A new methodology is proposed for the design of trajectory tracking controllers for autonomous vehicles. The design technique builds on gain scheduling control theory. An application is made to the design of a trajectory tracking controller for a prototype autonomous underwater vehicle (AUV). The effectiveness and advantages of the new control laws derived are illustrated in simulation using a full set of non-linear equations of motion of the vehicle. Copyright © 2002 John Wiley & Sons, Ltd.

KEY WORDS: guidance and control; trajectory tracking; gain-scheduled control; underwater vehicles

1. INTRODUCTION

Recently, there has been a surge of interest in the development of guidance and control systems for autonomous vehicles for accurate tracking of inertial reference trajectories. Practical applications include the operation of air, ground, and ocean vehicles for commercial and scientific purposes. See, for example, Reference [1] for a brief description of environmental and geological surveying missions using autonomous underwater vehicles (AUVs). See also References [2,3] for scientific missions that require the joint operation of air and underwater vehicles as well as the co-ordination of surface and underwater marine craft.

Traditionally, trajectory tracking controllers have been designed using the following methodology. First, an inner loop is designed to stabilize the vehicle dynamics. Then, using time-scale separation criteria, an outer loop is designed that relies essentially on the vehicle's kinematic model and converts tracking errors into inner loop commands. In classical and missile control literature this outer loop is usually referred to as a guidance loop, of which line of sight (LOS) guidance strategy is a typical example. See References [4–7] and the references therein for an introduction to the subject and for interesting applications to the control of air and underwater vehicles. Following this classical approach, control systems are designed based on

*Correspondence to: Carlos Silvestre, Department of Electrical Engineering and Computer Science and Institute for Systems and Robotics (ISR), Instituto Superior Tecnico, Av. Rovisco Pais, 1049-001 Lisbon, Portugal
[†] E-mail: cjs@isr.ist.utl.pt
[‡] E-mail: antonio@isr.ist.utl.pt
[§] E-mail: kaminer@aa.nps.navy.mil

vehicle dynamics, whereas guidance laws are essentially based on kinematic relationships only. During the design phase, a common rule of thumb is adopted whereby the control system is designed with sufficiently large bandwidth to track the commands that are expected from the guidance system (the so-called time-scale separation principle). However, since the two systems are effectively coupled, stability and adequate performance of the combined systems are not guaranteed. This potential problem is particularly serious in the case of underwater vehicles, which lack the agility of fast aircraft and thus impose tight restrictions on the closed loop bandwidths that can be achieved with any dynamic control law.

In practice, attempts to resolve this problem require the judicious choice of control bandwidth and guidance law parameters (such as so-called 'visibility distance' in the LOS strategy), guided by extensive computer simulations. Even when stability is obtained, however, the resulting guidance and control strategy may lead to finite trajectory tracking errors, the magnitude of which will depend on the type of trajectory to be tracked (radius of curvature, desired speed of the vehicle, etc.). See for example Reference [8] for an in-depth analysis of the stability of a combined guidance and control system for an AUV in the horizontal plane.

Motivated by the above considerations, this paper introduces a methodology for the design of guidance and control systems for autonomous vehicles whereby the two systems are designed simultaneously. This leads to a new class of trajectory tracking controllers that exhibit two major advantages over classical ones:

(i) stability of the combined guidance and control system is guaranteed, and
(ii) zero steady state error is achieved about any trimming trajectory.

The new design method builds on the following results that will be discussed later: (i) the trimming trajectories of autonomous vehicles correspond to helices parameterized by the vehicle's linear speed, yaw rate, and flight path angle (in the case of land or ocean surface vehicles, the trimming parameters are simply linear speed and yaw rate), (ii) tracking of a trimming trajectory by a vehicle is equivalent to driving a conveniently defined generalized tracking error to zero, and (iii) the linearization of the generalized error dynamics about any trimming trajectory is time invariant. Based on these results, the problem of integrated design of guidance and control systems for accurate tracking of trajectories that consist of the piecewise union of trimming trajectories can be cast in the framework of gain scheduled control theory. In this context, the vehicle's linear speed, yaw rate, and flight path angle play the role of scheduling variables that interpolate the parameters of linear controllers designed for a finite number of representative trimming trajectories.

There is a long history of gain scheduling in applications, namely in the areas of electro-mechanical systems, chemical process control, autopilots and flight control as well as automotive engine control. The reader will find [9] an excellent survey of the field, including latest theoretical developments. However, in spite of gain scheduling techniques having provided a fruitful set-up for the development and actual implementation of advanced control structures, considerable theoretical work must be done before a solid basis for stability and performance analysis will emerge. Current trends include casting gain scheduling control problems in the framework of linear parameter varying systems (LPV), linear fractional transformations (LFT), or even stability based switching theory, see Reference [9] and the references therein.

The main thrust of this paper is to show how the problem of trajectory tracking can be formulated as a gain scheduling control problem. Thus, it does not address explicitly the issues

of global stability and performance. Instead, the paper guides the reader through the steps that are commonly adopted in the design of a gain scheduled controller and shows clearly what procedures are required in the case of rigid body trajectory tracking control. As such, it illustrates the following classical steps in the development of a gain scheduled controller for a given plant [9,10]:

Linearizing the plant about a finite number of representative equilibrium (also referred to as operating) points and computing the respective linearizations. This step yields a parameterized family of linearized plants.

Designing linear controller for the linearized plants at each operating point. This produces a parameterized family of linear controllers that yield adequate stability and performance for the corresponding linearized models.

Interpolating the linear controllers in the previous step to achieve adequate performance of the linearized closed loop systems at all points where the plant is expected to operate. Interpolation is performed according to measurable scheduling variables that parameterize the plants equilibrium points.

Implementing the family of linear controllers such that the controller coefficients (gains) are varied (scheduled) according to the current values of the scheduling variables.

The last step requires considerable caution. In fact, ad-hoc methodologies for controller implementation will often lead to poor performance of even instability even at a local level. This is due to the presence of so-called hidden coupling [9,10]. To obviate this problem, an extension of so-called D-methodology [10] for the implementation of gain scheduled controllers is introduced in this paper. The resulting gain scheduled control law exhibits two main properties:

Linearization property—The linearization of the non-linear gain scheduled feedback control system about each trimming trajectory preserves the internal as well as the input–output properties of the corresponding linear closed loop designs.
Auto trimming property—The non-linear controller implementation does not require that the trimming values of all state variables and inputs be fed into the controller.

Surprisingly, the first property is often not satisfied by gain scheduled controllers proposed in the literature [10] due to the presence of hidden coupling. This paper shows how a simple implementation strategy overcomes this problem. The methodology is simple to apply and leads to a non-linear controller, the structure of which is similar to that of the original linear ones.

The second property is in striking contrast with most linearization based techniques for trajectory tracking proposed in the literature. In fact, the structure of the new non-linear tracking controllers is such that the trimming values for the plant inputs (as well as for the states variables that are not explicitly required to track kinematic reference inputs) are automatically acquired during operation.

The latter property can be easily understood by referring to the controller implementation methodology described in Reference [10] and extended in this paper for the case of trajectory tracking controllers. The methodology is based on the key observation that, in a gain scheduling setting, linear controllers are designed to operate on perturbations of the plant's inputs and

outputs about equilibrium points. Proper blending of the different controllers requires that they have access to such perturbations locally. This is achieved by differentiating some of the measured outputs before they are fed back to the gain scheduled controller. In order to preserve the input–output behaviour of the feedback system, integral action is provided at the input to the plant. The integrators hold the key to the success of the methodology, as they naturally 'charge up' to the input values required to trim the plant.

The paper starts by describing the general methodology adopted for the design of gain-scheduled trajectory tracking controllers. The techniques proposed are then applied to the design of a trajectory tracking controller for the prototype autonomous underwater vehicle (AUV) of Figure 8. The effectiveness and advantages of the resulting integrated guidance/control strategy are illustrated in simulation, using a full set of non-linear equations of motion of the vehicle.

It should be emphasized that the technique presented in this paper addresses precise tracking of trajectories defined in terms of space and time co-ordinates. This feature is important for many time-critical AUV missions. For the case where time is not of importance and the only requirement is that the vehicle follow a desired path, the reader is referred to Reference [11], as well as the excellent thesis by Al-Hibbabi [12] and references therein.

The paper is organized as follows. Section 2 presents the general form of the equations of motion of a rigid body and describes the computation of its trimming trajectories. Section 3 particularizes the results of Section 2 to the case of a prototype underwater vehicle and introduces a simple parameterization of its trimming trajectories as well as the corresponding relevant state and input variables. Section 4 introduces the definition of generalized tracking error and derives its time-invariant linearization about trimming trajectories. Section 5 formulates and describes a solution to the problem of trajectory tracking by casting it in the framework of gain scheduled control theory. Section 6 presents an alternative definition of generalized tracking error that simplifies controller implementation. Section 7 describes how the solution derived is applied to the design of a trajectory tracking controller for the Infante AUV, while Section 8 evaluates its performance using a non-linear simulation of the vehicle. Finally, Section 9 presents concluding remarks and Section 10 gives some useful notes on matrix properties.

2. RIGID BODY TRIMMING TRAJECTORIES

This section provides important basic notation, introduces the general form of the equations of motion of a rigid body subject to external forces and torques, and describes the computation of its equilibrium sets as well as trimming trajectories. The contents of the section have been strongly influenced by the work reported in Reference [13].

2.1. Rigid body dynamics

In what follows, it is assumed that the equations of motion of a rigid body can be written in standard form as

$$\frac{\mathrm{d}}{\mathrm{d}t}\mathbf{x} = \mathcal{F}(\mathbf{x}) + \mathcal{B}(\mathbf{x})\mathcal{H}(\mathbf{x}, \mathbf{u}) \tag{1}$$

where $\mathbf{x} \in \mathbb{R}^n$ and $\mathbf{u} \in \mathbb{R}^m$ are the state and input vectors, respectively and m is the number of actuators. The vector field $\mathcal{F}(\mathbf{x}) : \mathbb{R}^n \to \mathbb{R}^n$ represents the state dynamics, whereas $\mathcal{B}(\mathbf{x}) : \mathbb{R}^n \to \mathbb{R}^{n\times m}$ and $\mathcal{H}(\mathbf{x}, \mathbf{u}) : \mathbb{R}^{n+m} \to \mathbb{R}^m$ describe the effect of the rigid body actuators on the state. It is assumed that $\mathcal{B}(\mathbf{x})$ has full rank. Notice that Equations (1) are restricted to be affine on the term $\mathcal{H}(\mathbf{x}, \mathbf{u})$ that involves inputs. However, they do capture the most important phenomena involved in the motion of a large class of air, ground, and marine vehicles.

Often, the equations of motion (1) arise from higher order (that is, greater than first order) differential equations. In this case, the equations can be split into two different sets that are usually referred to as 'dynamics' and 'kinematics'. Dynamics refers to the relationship between the highest order derivatives and the physical forces and torques applied to the rigid body. Kinematics refers to the analytic relationships between the derivatives of various orders, and these are independent of any exogenous input variables.

Using the separation between 'dynamics' and 'kinematics' and defining

$$\mathbf{x} := \begin{bmatrix} \mathbf{x}_{\text{dyn}} \\ \mathbf{x}_{\text{kin}} \end{bmatrix}; \quad \mathbf{x}_{\text{dyn}} \in \mathbb{R}^k, \mathbf{x}_{\text{kin}} \in \mathbb{R}^p \tag{2}$$

it follows that Equation (1) can be written as

$$\frac{\mathrm{d}}{\mathrm{d}t}\begin{bmatrix} \mathbf{x}_{\text{dyn}} \\ \mathbf{x}_{\text{kin}} \end{bmatrix} = \begin{bmatrix} \mathcal{F}_{\text{dyn}}(\mathbf{x}_{\text{dyn}}, \mathbf{x}_{\text{kin}}) \\ \mathcal{F}_{\text{kin}}(\mathbf{x}_{\text{dyn}}, \mathbf{x}_{\text{kin}}) \end{bmatrix} + \begin{bmatrix} \mathcal{B}(\mathbf{x}_{\text{dyn}})\mathcal{H}(\mathbf{x}_{\text{dyn}}, \mathbf{u}) \\ 0 \end{bmatrix} \tag{3}$$

where the first k equations represent the rigid body dynamics and the last p equations represent the kinematics. Notice the practical assumption that $\mathcal{B}(\mathbf{x})$ and $\mathcal{H}(\mathbf{x}, \mathbf{u})$ do not depend on $\mathbf{x}_{\text{kin}}$.

2.2. Equilibrium sets

The linearization method adopted in this work requires the computation of the equilibrium points of dynamical systems described by ordinary differential equations of the form

$$\frac{\mathrm{d}}{\mathrm{d}t}\mathbf{x} = f(\mathbf{x}, \mathbf{u}) \tag{4}$$

where $\mathbf{x} \in \mathbb{R}^n$ is the state, $\mathbf{u} \in \mathbb{R}^m$ is the input, and $f : \mathbb{R}^{n+m} \to \mathbb{R}^n$. Given the dynamical system (4),

$$E := \{(\mathbf{x}, \mathbf{u}) \in \mathbb{R}^{n+m} : \ f(\mathbf{x}, \mathbf{u}) = 0\}$$

denotes it *equilibrium set* and

$$E_s := \{\mathbf{x} : \ \exists \mathbf{u} \in \mathbb{R}^m, (\mathbf{x}, \mathbf{u}) \in E\}$$

is the corresponding *state equilibrium set*.

Suppose the system of Equations (4) does not depend on $\mathbf{u}$. Under fairly general conditions, the corresponding set E is a manifold of dimension $0 \leqslant l \leqslant n$. Typically, E consists of isolated equilibrium points, in which case the manifold has dimension $l = 0$. Suppose now that one control input is added, that is, $m = 1$. Then, for each value of the input $\mathbf{u}$, there will be, in general, a corresponding set of isolated equilibrium points. Furthermore, the family of equilibrium points generated in this manner will be such that E_s is a one-dimensional set. Similarly, systems with m inputs will typically have sets E_s of dimension m. Under very general conditions on the vector field f the set E_s is a smooth mathematical set called an 'm-dimensional manifold'.

The computation of the equilibrium set or the state equilibrium set of a rigid body depends on the structure of its kinematic and dynamic equations. See for example Reference [14] for an introduction to this subject and [13] for the computation of the state equilibrium manifold for a 6 degree-of-freedom aircraft model. As will become clear later, in the problems tackled in this paper the kinematic variables can be split into two sets, that is,

$$\mathbf{x}_{\text{kin}} = [\mathbf{x}_{\text{kin},i}^{\text{T}}, \mathbf{x}_{\text{kin},o}^{\text{T}}]^{\text{T}} \tag{5}$$

where $\mathbf{x}_{\text{kin},i} \in \mathbb{R}^q$ denotes the kinematic variables that appear explicitly in the top equations of (3) and $\mathbf{x}_{\text{kin},o} \in \mathbb{R}^{p-q}$ are the remaining variables. Using this nomenclature, Equations (3) can be rewritten as

$$\frac{\text{d}}{\text{d}t}\begin{bmatrix} \mathbf{x}_{\text{dyn}} \\ \mathbf{x}_{\text{kin},i} \\ \mathbf{x}_{\text{kin},o} \end{bmatrix} = \begin{bmatrix} \mathcal{F}_{\text{dyn}}(\mathbf{x}_{\text{dyn}}, \mathbf{x}_{\text{kin},i}) \\ \mathcal{F}_{\text{kin},i}(\mathbf{x}_{\text{dyn}}, \mathbf{x}_{\text{kin},i}) \\ \mathcal{F}_{\text{kin},o}(\mathbf{x}_{\text{dyn}}, \mathbf{x}_{\text{kin}}) \end{bmatrix} + \begin{bmatrix} \mathcal{B}(\mathbf{x}_{\text{dyn}})\mathcal{H}(\mathbf{x}_{\text{dyn}}, \mathbf{u}) \\ 0 \\ 0 \end{bmatrix} \tag{6}$$

where it is assumed that the kinematic equations for $\mathbf{x}_{\text{kin},i}$ do not depend on $\mathbf{x}_{\text{kin},o}$. Henceforth, the equilibrium set E^r of a rigid body described by Equations (6) is defined as

$$E^r \coloneqq \left\{ (\mathbf{x}_{\text{dyn}}, \mathbf{x}_{\text{kin},i}, \mathbf{u}) \in \mathbb{R}^{k+q+m} : \begin{bmatrix} \mathcal{F}_{\text{dyn}}(\mathbf{x}_{\text{dyn}}, \mathbf{x}_{\text{kin},i}) \\ \mathcal{F}_{\text{kin},i}(\mathbf{x}_{\text{dyn}}, \mathbf{x}_{\text{kin},i}) \end{bmatrix} + \begin{bmatrix} \mathcal{B}(\mathbf{x}_{\text{dyn}})\mathcal{H}(\mathbf{x}_{\text{dyn}}, \mathbf{u}) \\ 0 \end{bmatrix} = \begin{bmatrix} 0 \\ 0 \end{bmatrix}. \right\} \tag{7}$$

Notice how the kinematic equations for $\mathbf{x}_{\text{kin},o}$ do not play a role in the definition of the set E^r. Similarly, the state equilibrium set E_s^r of a rigid body is defined as

$$E_s^r \coloneqq \{(\mathbf{x}_{\text{dyn}}, \mathbf{x}_{\text{kin},i}) \in \mathbb{R}^{k+q} : \exists \mathbf{u} \in \mathbb{R}^m, (\mathbf{x}_{\text{dyn}}, \mathbf{x}_{\text{kin},i}, \mathbf{u}) \in E\}$$

The main focus of this section is on the computation of the equilibrium sets E^r, that is, finding solutions to the equations

$$\begin{bmatrix} \mathcal{F}_{\text{dyn}}(\mathbf{x}_{\text{dyn}}, \mathbf{x}_{\text{kin},i}) \\ \mathcal{F}_{\text{kin},i}(\mathbf{x}_{\text{dyn}}, \mathbf{x}_{\text{kin},i}) \end{bmatrix} + \begin{bmatrix} \mathcal{B}(\mathbf{x}_{\text{dyn}})\mathcal{H}(\mathbf{x}_{\text{dyn}}, \mathbf{u}) \\ 0 \end{bmatrix} = \begin{bmatrix} 0 \\ 0 \end{bmatrix} \tag{8}$$

At this point it is important to emphasize that the above equation is affine in $\mathcal{H}(\mathbf{x}_{\text{dyn}}, \mathbf{u})$. This allows eliminating the input variable $\mathbf{u}$ from the non-linear system of Equations (8) by pre-multiplying the top equation by the $k - m$ by k orthogonal complement $\mathcal{B}^{\perp}(\mathbf{x}_{\text{dyn}})$ of $\mathcal{B}(\mathbf{x}_{\text{dyn}})$ that satisfies the relationship [13]

$$\mathcal{B}^{\perp}(\mathbf{x}_{\text{dyn}})\mathcal{B}(\mathbf{x}_{\text{dyn}}) = 0, \quad \mathcal{B}^{\perp}(\mathbf{x}_{\text{dyn}}) \in \mathbb{R}^{(k-m)\times k}$$

This yields the system of equations

$$\begin{aligned} \mathcal{B}^{\perp}(\mathbf{x}_{\text{dyn}})\mathcal{F}_{\text{dyn}}(\mathbf{x}_{\text{dyn}}, \mathbf{x}_{\text{kin},i}) &= 0 \\ \mathcal{F}_{\text{kin},i}(\mathbf{x}_{\text{dyn}}, \mathbf{x}_{\text{kin},i}) &= 0 \end{aligned} \tag{9}$$

which corresponds to $k + q - m$ equations in the $k + q$ unknowns $\mathbf{x}_{\text{dyn}}$ and $\mathbf{x}_{\text{kin},i}$. The operator $\mathcal{B}^{\perp}(\mathbf{x}_{\text{dyn}})$ is not unique. Particular solutions derived using the fact that $\mathcal{B}^{\perp}(\mathbf{x}_{\text{dyn}})$ is full rank can be found in References [13,14].

In general, the set of solutions of (9) (that is, the state equilibrium set E_s^r) has dimension m. Suppose that the q kinematic equations can be used to eliminate q of the variables, leaving only k unknowns, denoted $\mathbf{x}_{\text{eq}}$. In this case, one is left with a system of $k-m$ equations

$$\mathcal{B}^{\perp}(\mathbf{x}_{\text{eq}})\mathcal{F}_{\text{dyn}}(\mathbf{x}_{\text{eq}}) = 0 \tag{10}$$

in the k variables $\mathbf{x}_{\text{eq}}$. A system of $k-m$ equations in k variables has an m-dimensional solution set.

Additional constraints are thus necessary to obtain a unique solution. The constraints are problem-dependent and require examining the structure of the kinematic equations for $\mathbf{x}_{\text{kin},o}$, as well as the possible types of so-called trimming trajectories for the rigid body in question. An example will be presented later. A technique to compute the remaining q components of $\mathbf{x}$ as well as the input vector $\mathbf{u}$ can be found in Reference [14].

2.3. Trimming trajectories

The concept of trimming trajectory of a rigid body is closely related to that of its equilibrium set E^r.

Definition 2.1 (*Generalized trimming trajectory*)
Given a rigid body $\bar{\mathcal{R}}$ with dynamics (1) and equilibrium set E^r, a generalized trimming trajectory Υ_C^g of $\bar{\mathcal{R}}$ is defined as

$$\Upsilon_C^g := \{(\mathbf{x}_{\text{dyn}_C}, \mathbf{x}_{\text{kin}_C}(\cdot), \mathbf{u}_C) : (\mathbf{x}_{\text{dyn}_C}, \mathbf{x}_{\text{kin},i_C}, \mathbf{u}_C) \in E^r\} \tag{11}$$

where $\mathbf{x}_{\text{dyn}_C} \in \mathbb{R}^k$, $\mathbf{x}_{\text{kin}_C}(\cdot) : \mathbb{R}_+ \to \mathbb{R}^p$, and $\mathbf{u}_C \in \mathbb{R}^m$. The vector $[\mathbf{x}_{\text{dyn}_C}^{\text{T}}, \mathbf{x}_{\text{kin},i_C}^{\text{T}}, \mathbf{u}_C^{\text{T}}]^{\text{T}} \in \mathbb{R}^{k+q+m}$ is called the trimming vector of Υ_C^g.

Notice in the definition that $\mathbf{x}_{\text{kin}_C}$ is allowed to be a function of time. For example, in the case of an aircraft at trimmed level flight, the inertial position co-ordinates change with time.

The following definitions are also required.

Definition 2.2 (*Trimming trajectory*)
Given a rigid body $\bar{\mathcal{R}}$ with dynamics (1), a trimming trajectory Υ_C of $\bar{\mathcal{R}}$ is defined as

$$\Upsilon_C := \{\mathbf{x}_{\text{kin}_C}(\cdot) : \exists \Upsilon_C^g, \mathbf{x}_{\text{kin}_C}(\cdot) = \Pi_k \Upsilon_C^g\} \tag{12}$$

where Υ_C^g is a generalized trimming trajectory of $\bar{\mathcal{R}}$ and $\Pi_k \Upsilon_C^g$ is the operator that extracts the (kinematic) $\mathbf{x}_{\text{kin}_C}(\cdot)$ components from Υ_C^g. The vector $[\mathbf{x}_{\text{dyn}_C}^{\text{T}}, \mathbf{x}_{\text{kin},i_C}^{\text{T}}, \mathbf{u}_C^{\text{T}}]^{\text{T}} \in \mathbb{R}^{k+q+m}$ is called the trimming vector of Υ_C.

It is important to point out that the trimming trajectories of a rigid body include its kinematic variables only.

A trimming trajectory of a rigid body or vehicle moving in a flow field corresponds to the situation where all the inputs are fixed and the dynamic variables $\mathbf{x}_{\text{dyn}}$ are constant. Furthermore, at trimming the kinematic variables $\mathbf{x}_{\text{kin},i}$ must also be constant. Thus, at trimming

$$0 = \mathcal{F}_{\text{dyn}}(\mathbf{x}_{\text{dyn}_C}, \mathbf{x}_{\text{kin},i_C}) + \mathcal{B}(\mathbf{x}_{\text{dyn}_C})\mathcal{H}(\mathbf{x}_{\text{dyn}_C}, \mathbf{u}_C) \tag{13}$$

Definition 2.3 (*Set of trimming trajectories* $\mathcal{E}$)
Given a rigid body $\bar{\mathcal{R}}$ with dynamics (1), the set of trimming trajectories $\mathcal{E}$ of $\bar{\mathcal{R}}$ is defined as the collection of all its trimming trajectories Υ_C.

3. AUV DYNAMICAL MODEL AND TRIMMING TRAJECTORIES

This section presents the equations of motion of an autonomous underwater vehicle (AUV) (see Figure 8) and casts them in the general form introduced in Section 2. The equilibrium (also called trimming) trajectories of the vehicle are derived and parameterized. The corresponding trimming vectors are computed.

3.1. Underwater vehicle dynamics

The equations of motion for underwater vehicles can be obtained from Newton–Euler and hydrodynamic laws following the classical approach described in Reference [15]. With this set-up, the equations are easily developed using a inertial co-ordinate frame $\{I\}$ and a body fixed co-ordinate frame $\{B\}$ that moves with the AUV. Due to space limitation only the general form of the equations is described here. See for example References [16,17] for complete details and basic nomenclature. The following notation is required:

$\mathbf{p} = [x, y, z]^{\mathrm{T}}$—position of the origin of $\{B\}$ expressed in $\{I\}$;
$\mathbf{v} = [u, v, w]^{\mathrm{T}}$—linear velocity of the origin of $\{B\}$ relative to $\{I\}$, expressed in $\{B\}$;
$\boldsymbol{\lambda} = [\phi, \theta, \psi]^{\mathrm{T}}$—vector of Euler angles (roll, pitch, and yaw) that describes the orientation of frame $\{B\}$ with respect to $\{I\}$;
$\boldsymbol{\omega} = [p, q, \tau]^{\mathrm{T}}$—body fixed angular velocity of $\{B\}$ relative to $\{I\}$, expressed in $\{B\}$;
$\mathcal{R} = {}^{I}_{B}R(\boldsymbol{\lambda})$—rotation matrix from $\{B\}$ to $\{I\}$, parameterized locally by $\boldsymbol{\lambda}$; $\mathcal{R}$ is orthonormal, and $\mathcal{R} = I$ for $\boldsymbol{\lambda} = 0$;
$\mathcal{Q} = Q(\boldsymbol{\lambda})$—matrix that relates body fixed angular velocity $\boldsymbol{\omega}$ to Euler angles rates; $\mathcal{Q}$ satisfies $\dot{\boldsymbol{\lambda}} = \mathcal{Q}\boldsymbol{\omega}$ and equals the identity for $\boldsymbol{\lambda} = 0$.
Let

$$\mathbf{x}_{\mathrm{dyn}} \equiv \begin{bmatrix} \mathbf{v} \\ \boldsymbol{\omega} \end{bmatrix}, \quad \mathbf{x}_{\mathrm{kin}} \equiv \begin{bmatrix} \mathbf{p} \\ \boldsymbol{\lambda} \end{bmatrix} \tag{14}$$

where $\mathbf{x}_{\mathrm{dyn}} \in \mathbb{R}^6$ and $\mathbf{x}_{\mathrm{kin}} \in \mathbb{R}^6$ denote the dynamic and kinematic variables that are used to describe the complete motion of the vehicle. Further, let

$$L(\boldsymbol{\lambda}) \equiv \begin{bmatrix} \mathcal{R} & 0 \\ 0 & \mathcal{Q} \end{bmatrix}$$

Using the above notation, the vehicle dynamics and kinematics can be described by (see Reference [13] for the case of aircraft and Reference [14] for underwater vehicles):

$$M_{\mathrm{RB}} \frac{\mathrm{d}}{\mathrm{d}t}\mathbf{x}_{\mathrm{dyn}} + C_{\mathrm{RB}}(\mathbf{x}_{\mathrm{dyn}})\mathbf{x}_{\mathrm{dyn}} = \boldsymbol{\tau}\left(\frac{\mathrm{d}}{\mathrm{d}t}\mathbf{x}_{\mathrm{dyn}}, \mathbf{x}_{\mathrm{dyn}}, \boldsymbol{\lambda}, \boldsymbol{\delta}, n\right) \tag{15}$$

$$\frac{\mathrm{d}}{\mathrm{d}t}\mathbf{x}_{\mathrm{kin}} = L(\boldsymbol{\lambda})\mathbf{x}_{\mathrm{dyn}} \tag{16}$$

where $\boldsymbol{\tau}$ denotes the vector of external forces and moments, and M_{RB} and C_{RB} denote the rigid body inertia matrix and the matrix of Coriolis and centrifugal terms, respectively. The vector $\boldsymbol{\tau}$ can be further decomposed as

$$\boldsymbol{\tau}\left(\frac{\mathrm{d}}{\mathrm{d}t}\mathbf{x}_{\mathrm{dyn}}, \mathbf{x}_{\mathrm{dyn}}, \boldsymbol{\lambda}, \boldsymbol{\delta}, n\right) = \boldsymbol{\tau}_{\mathrm{rest}}(\boldsymbol{\lambda}) + \boldsymbol{\tau}_{\mathrm{add}}\left(\frac{\mathrm{d}}{\mathrm{d}t}\mathbf{x}_{\mathrm{dyn}}, \mathbf{x}_{\mathrm{dyn}}\right) + \boldsymbol{\tau}_{\mathrm{surf}}(\mathbf{x}_{\mathrm{dyn}}, \boldsymbol{\delta}) + \boldsymbol{\tau}_{\mathrm{visc}}(\mathbf{x}_{\mathrm{dyn}}, \boldsymbol{\delta}) + \tau_{\mathrm{prop}}(\mathbf{x}_{\mathrm{dyn}}, n) \tag{17}$$

where $\boldsymbol{\tau}_{\mathrm{rest}}$ consists of the (restoring) forces and moments caused by the interplay between gravity and buoyancy, and $\boldsymbol{\tau}_{\mathrm{add}}$ is the added mass term. The term $\boldsymbol{\tau}_{\mathrm{surf}}$ captures the forces and moments generated by the deflecting surfaces, $\boldsymbol{\tau}_{\mathrm{visc}}$ consists of the hydrodynamic forces and moments exerted on the vehicle's body (including the skin friction terms), and $\boldsymbol{\tau}_{\mathrm{prop}}$ represents the forces and moments generated by the main propellers. The input vector $\boldsymbol{\delta} = [\delta_{\mathrm{d}}, \delta_{\mathrm{b}}, \delta_{\mathrm{s}}, \delta_{\mathrm{r}}]^{\mathrm{T}}$ consists of the differential mode of the bow and stern plane deflections, common mode bow plane deflection, common mode stern plane deflection and deflections of the rudders, respectively. The symbol n denotes the speed of rotation of the main propellers.

It is now routine to rewrite Equations (15) and(16) in the standard state-space form of (3) as

$$\mathcal{P} = \begin{cases} \dfrac{\mathrm{d}}{\mathrm{d}t}\mathbf{x}_{\mathrm{dyn}} = \mathcal{F}_{\mathrm{dyn}}(\mathbf{x}_{\mathrm{dyn}}, \mathbf{x}_{\mathrm{kin}}) + \mathcal{B}(\mathbf{x}_{\mathrm{dyn}})\mathcal{H}(\mathbf{x}_{\mathrm{dyn}}, \mathbf{u}) \\ \dfrac{\mathrm{d}}{\mathrm{d}t}\mathbf{x}_{\mathrm{kin}} = L(\boldsymbol{\lambda})\mathbf{x}_{\mathrm{dyn}} \end{cases} \tag{18}$$

by making

$$\mathbf{u} = [\boldsymbol{\delta}^{\mathrm{T}}, \mathbf{n}]^{\mathrm{T}} \tag{19}$$

and

$$\mathcal{F}_{\mathrm{kin}}(\mathbf{x}_{\mathrm{dyn}}, \mathbf{x}_{\mathrm{kin}}) = L(\boldsymbol{\lambda})\mathbf{x}_{\mathrm{dyn}} \tag{20}$$

Physical considerations dictate that $\mathcal{F}_{\mathrm{dyn}}$ depends on the kinematic variables $\phi, \theta \in \boldsymbol{\lambda}$ but not on ψ and $\mathbf{p}$. This means that the dynamics of the underwater vehicle are independent of its linear position in space and its yaw angle. Furthermore, the matrix $\mathcal{Q}$ does not depend on the angle ψ. To simplify the physical interpretation of the variables involved in the vehicle's model (18) can be written in expanded form as

$$\mathcal{P} = \begin{cases} \dfrac{\mathrm{d}}{\mathrm{d}t}\mathbf{v} = \mathcal{F}_{\mathbf{v}}(\mathbf{v}, \boldsymbol{\omega}) + \mathcal{F}_{\mathbf{v}}^{\boldsymbol{\lambda}}(\Pi_i\boldsymbol{\lambda}) + \mathcal{B}_{\mathbf{v}}(\mathbf{v}, \boldsymbol{\omega})\mathcal{H}(\mathbf{v}, \mathbf{u}) \\ \dfrac{\mathrm{d}}{\mathrm{d}t}\boldsymbol{\omega} = \mathcal{F}_{\boldsymbol{\omega}}(\mathbf{v}, \boldsymbol{\omega}) + \mathcal{F}_{\boldsymbol{\omega}}^{\boldsymbol{\lambda}}(\Pi_i\boldsymbol{\lambda}) + \mathcal{B}_{\boldsymbol{\omega}}(\mathbf{v}, \boldsymbol{\omega})\mathcal{H}(\mathbf{v}, \mathbf{u}) \\ \dfrac{\mathrm{d}}{\mathrm{d}t}\mathbf{p} = \mathcal{R}(\boldsymbol{\lambda})\mathbf{v} \\ \dfrac{\mathrm{d}}{\mathrm{d}t}\boldsymbol{\lambda} = \mathcal{Q}(\Pi_i\boldsymbol{\lambda})\boldsymbol{\omega} \end{cases} \tag{21}$$

where the functions, $\mathcal{F}_{\mathbf{v}}$, $\mathcal{F}_{\mathbf{v}}^{\boldsymbol{\lambda}}$, $\mathcal{B}_{\mathbf{v}}$, $\mathcal{F}_{\boldsymbol{\omega}}$, $\mathcal{F}_{\boldsymbol{\omega}}^{\boldsymbol{\lambda}}$ and $\mathcal{B}_{\boldsymbol{\omega}}$ are obtained from $\mathcal{F}$ and $\mathcal{B}$ and $\Pi_i\boldsymbol{\lambda} = [\phi, \theta]^{\mathrm{T}}$. Often, and with an obvious abuse of notation, $\mathcal{F}_{\mathbf{v}}^{\boldsymbol{\lambda}}(\Pi_i\boldsymbol{\lambda}), \mathcal{F}_{\boldsymbol{\omega}}^{\boldsymbol{\lambda}}(\Pi_i\boldsymbol{\lambda})$, and $\mathcal{Q}(\Pi_i\boldsymbol{\lambda})$, will be simply written as $\mathcal{F}_{\mathbf{v}}^{\boldsymbol{\lambda}}(\boldsymbol{\lambda})$, $\mathcal{F}_{\boldsymbol{\omega}}^{\boldsymbol{\lambda}}(\boldsymbol{\lambda})$, and $\mathcal{Q}(\boldsymbol{\lambda})$, respectively.

The dependence of $\mathcal{F}_{\text{dyn}}$ on ϕ and θ shows up in the force and torque terms that arise due to the interplay between gravity and buoyancy forces, which can be further decomposed as

$$\mathcal{F}_{\mathbf{v}}^{\lambda}(\boldsymbol{\lambda}) = M_{\mathbf{v}}\mathcal{R}^{-1}\mathbf{g}, \quad \mathcal{F}_{\boldsymbol{\omega}}^{\lambda}(\boldsymbol{\lambda}) = M_{\boldsymbol{\omega}}\mathcal{R}^{-1}\mathbf{g}$$

where

$$\mathbf{g} = [0, 0, g]^{\mathrm{T}}$$

is the gravity acceleration vector expressed in the inertial co-ordinate system and matrices $M_{\mathbf{v}}$ and $M_{\boldsymbol{\omega}}$ are obtained from the vehicle's physical parameters [14]. From the above discussion it follows immediately that

$$\mathbf{x}_{\text{kin},i} = [\phi, \theta]^{\mathrm{T}} \tag{22}$$

and

$$\mathbf{x}_{\text{kin},o} = [\psi, \mathbf{p}^{\mathrm{T}}]^{\mathrm{T}} \tag{23}$$

In this case the set of trimming trajectories of the AUV is easily seen to be of the form

$$\mathcal{E} := \left\{ \begin{array}{ll} \mathbf{x}_{\text{kin}_C}(.) = \begin{bmatrix} \mathbf{p}_C(.) \\ \boldsymbol{\lambda}_C(.) \end{bmatrix} : & \dfrac{\mathrm{d}}{\mathrm{d}t}\mathbf{p}_C(.) = \mathcal{R}_C(\boldsymbol{\lambda}_C(.))\mathbf{v}_C, \\ & \dfrac{\mathrm{d}}{\mathrm{d}t}\boldsymbol{\lambda}_C(.) = \mathcal{Q}_C(\Pi_i\boldsymbol{\lambda}_C(.))\boldsymbol{\omega}_C, \\ & \mathcal{F}_{\mathbf{v}}(\mathbf{v}_C, \boldsymbol{\omega}_C) + \mathcal{F}_{\mathbf{v}}^{\lambda}(\Pi_i\boldsymbol{\lambda}_C(.)) + \mathcal{B}_{\mathbf{v}}(\mathbf{v}_C, \boldsymbol{\omega}_C)\mathcal{H}(\mathbf{v}_C, \mathbf{u}_C) = 0, \\ & \mathcal{F}_{\boldsymbol{\omega}}(\mathbf{v}_C, \boldsymbol{\omega}_C) + \mathcal{F}_{\boldsymbol{\omega}}^{\lambda}(\Pi_i\boldsymbol{\lambda}_C(.)) + \mathcal{B}_{\boldsymbol{\omega}}(\mathbf{v}_C, \boldsymbol{\omega}_C)\mathcal{H}(\mathbf{v}_C, \mathbf{u}_C) = 0 \end{array} \right\} \tag{24}$$

where $\mathbf{v}_C$, $\boldsymbol{\omega}_C$, $\mathbf{u}_C$ and $\Pi_i\boldsymbol{\lambda}_C = [\phi_C, \theta_C]^{\mathrm{T}}$ denote trimming values of $\mathbf{v}, \boldsymbol{\omega}, \mathbf{u}$ and $\Pi\boldsymbol{\lambda}$, respectively. Clearly, $[\mathbf{v}_C^{\mathrm{T}}, \boldsymbol{\omega}_C^{\mathrm{T}}, \Pi_i\boldsymbol{\lambda}^{\mathrm{T}}, \mathbf{u}_C^{\mathrm{T}}]^{\mathrm{T}}$ is the trimming vector of an element of $\mathcal{E}$. In practice, the trimming vector is restricted to be in some compact set.

As explained later, it is natural to attach to each trimming trajectory Υ_C of a rigid body a body fixed co-ordinate system $\{C\}$ that describes the position and orientation of the body along that trajectory. In this case, the variables introduced before have the following interpretation:

$\mathbf{p}_C$—position of the origin of $\{C\}$ expressed in $\{I\}$;
$\mathbf{v}_C$—linear velocity of the origin of $\{C\}$ relative to $\{I\}$ expressed in $\{C\}$;
$\boldsymbol{\lambda}_C$—Vector of Euler angles which describes the orientation of frame $\{C\}$ in $\{I\}$;
$\boldsymbol{\omega}_C$—angular velocity of $\{C\}$ relative to $\{I\}$ expressed in $\{C\}$.
In preparation for the section that follows it is convenient to define
$\mathcal{R}_C = {}_C^I\mathcal{R}(\boldsymbol{\lambda}_C(t))$—rotation matrix from $\{C\}$ to $\{I\}$;
$\mathcal{Q}_C = \mathcal{Q}(\boldsymbol{\lambda}_C(t))$.

It is assumed that the reader is familiar with the definitions of angle of attack $\alpha = \arcsin(w/(u^2 + w^2)^{1/2})$, sideslip angle $\beta = \arcsin(v/(u^2 + v^2 + w^2)^{1/2})$, and flight path angle γ, as well as the concept of flow frame (usually referred to as wind frame in aeronautics). See Reference [6].

3.2. Trimming trajectories parameterization

At trimming, the body referenced linear and angular velocities $\mathbf{v}$ and $\boldsymbol{\omega}$ and the roll and pitch angles are constant, that is,

$$\frac{\mathrm{d}}{\mathrm{d}t}\mathbf{x}_{\mathrm{dyn}} = \frac{\mathrm{d}}{\mathrm{d}t}[\mathbf{v}^{\mathrm{T}}, \boldsymbol{\omega}^{\mathrm{T}}]^{\mathrm{T}} = 0, \quad \frac{\mathrm{d}}{\mathrm{d}t}\mathbf{x}_{\mathrm{kin},i} = \frac{\mathrm{d}}{\mathrm{d}t}[\phi, \theta]^{\mathrm{T}} = 0 \tag{25}$$

Let $\mathbf{v}_C$, $\boldsymbol{\omega}_C$, ϕ_C, and θ_C denote the trimming values of $\mathbf{v}$, $\boldsymbol{\omega}$, ϕ, and θ respectively. In References [13,14] it is shown that

$$\frac{\mathrm{d}}{\mathrm{d}t}\begin{bmatrix} x_C \\ y_C \\ z_C \end{bmatrix} = \begin{bmatrix} \mathbf{V}_{\tau_c}\cos(\gamma_C)\cos(\dot{\psi}_C t + \psi_o) \\ \mathbf{V}_{\tau_c}\cos(\gamma_C)\sin(\dot{\psi}_C t + \psi_o) \\ -\mathbf{V}_{\tau_c}\sin(\gamma_C) \end{bmatrix} \tag{26}$$

where $\dot{\psi}_C$ is yaw rate, ψ_v denotes the angle between the vehicle heading and the vehicle velocity vector, $\mathbf{V}_{\tau_c} = \|\mathbf{v}_C\|$ is linear body speed, and γ_C is the so-called 'trimming flight path angle'.

Integrating the above equation shows that the only possible trimming trajectories $\Upsilon_C \in \mathcal{E}$ of the underwater vehicle correspond to helices described by

$$\boldsymbol{\lambda}_C(t) = \begin{bmatrix} \phi_C \\ \theta_C \\ \dot{\psi}_C t + \psi_v + \psi_0 \end{bmatrix}, \quad \mathbf{p}_C(t) = \begin{bmatrix} \frac{\mathbf{v}_{\tau_c}}{\psi_C}\cos(\gamma_C)\sin(\dot{\psi}_C t + \psi_o) \\ \frac{\mathbf{v}_{\tau_c}}{\psi_C}\cos(\gamma_C)\cos(\dot{\psi}_C t + \psi_o) \\ -\mathbf{V}_{\tau_c}\sin(\gamma_C)t \end{bmatrix} + \begin{bmatrix} x_0 \\ y_0 \\ z_0 \end{bmatrix} \tag{27}$$

where the vector $[x_0, y_0, z_0]^{\mathrm{T}}$ and ψ_0 denote the helix initial conditions (see Figure 1).

It can thus be concluded that the set $\mathcal{E}$ of trimming trajectories can be completely parametrized by the vector

$$\boldsymbol{\eta}_C = [\mathbf{V}_{\tau_c},\ \dot{\psi}_C, \gamma_C] \in \mathbb{R}^3 \tag{28}$$

Given a trimming trajectory Γ_C parameterized by $\boldsymbol{\eta}_C$ and an AUV dynamic model (21) one is now faced with the problem of actually computing the state and control vectors that satisfy these equations, that is, the trimming vector of Γ_C. This step is problem dependent and builds on the algorithm introduced in Section 2 for the computation of the rigid body equilibrium set. In the case of the AUV under consideration, the constraints that follow are sufficient to completely specify the trimming vector as a function of $\boldsymbol{\eta}_C$, thus showing that *the trimming vector is parameterized by* $\boldsymbol{\eta}_C$. See Reference [14] for further details.

3.2.1. Constraint on linear velocity

The parameter $\mathbf{V}_{\tau_c}$ imposes the constraint

$$\|\mathbf{v}_C\| = \mathbf{V}_{T_c}$$

on the vehicle's velocity vector $\mathbf{v}$. It is straightforward to show that

$$\mathbf{v}_C = \begin{bmatrix} u_C \\ v_C \\ w_C \end{bmatrix} = \begin{bmatrix} \mathbf{V}_{T_c}\cos(\alpha_C)\cos(\beta_C) \\ \mathbf{V}_{T_c}\sin(\beta_C) \\ \mathbf{V}_{T_c}\sin(\alpha_C)\cos(\beta_C) \end{bmatrix}$$

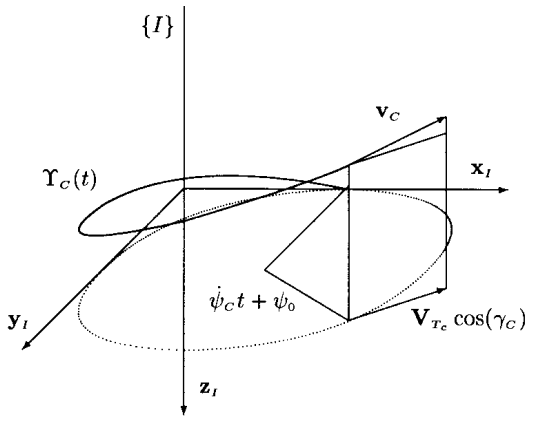

Figure 1. Trimming trajectory.

where the angles of attack α_C and sideslip β_C are constant and remain free to accommodate extra constraints.

3.2.2. Constraint on rate of climb

In Equation (26), the rate of climbing at trimming is simply

$$\dot{\mathbf{z}}_{IC} = -\mathbf{V}_{T_c} \sin(\gamma_C)$$

which corresponds to the negative z-axis component of the vehicle velocity vector expressed in the inertial frame $\{I\}$. One can now use a co-ordinate transformation from the flow axes to the inertial co-ordinate system to obtain an extra constraint as follows. Start by writing

$$\begin{bmatrix} \mathbf{V}_{T_c} \cos(\gamma_C) \cos(\dot{\psi}_C t + \psi_o) \\ \mathbf{V}_{T_c} \cos(\gamma_C) \sin(\dot{\psi}_C t + \psi_o) \\ -\mathbf{V}_{T_c} \sin(\gamma_C) \end{bmatrix} = \mathcal{R}\mathcal{R}_F^T \begin{bmatrix} \mathbf{V}_{T_c} \\ 0 \\ 0 \end{bmatrix}$$

where $\mathcal{R}_F$ (which is a function of angles of attack and sideslip) is the rotation matrix from flow to body axis. Notice the important fact that when written in the flow axis only the first component of the total velocity vector is different from zero. This equation can be expanded and arranged to give

$$\begin{aligned} \sin(\gamma_C) = {} & \cos(\alpha_C) \cos(\beta_C) \sin(\theta_C) \\ & - [\sin(\phi_C) \sin(\beta_C) + \cos(\phi_C) \sin(\alpha_C) \cos(\beta_C)] \cos(\theta_C) \end{aligned} \tag{29}$$

which is the required constraint. If $\phi_C = 0$ and $\beta_C = 0$, this leads to the well known relationship

$$\theta_C = \alpha_C + \gamma_C$$

that is, pitch angle is equal to the sum of flight path angle and angle of attack.

3.2.3. Constraint on angle of attack

Due to the existence of bow and stern control surfaces, the AUV is capable of performing steady state manoeuvres in the vertical plane with an arbitrary angle of attack α_C. Thus, an additional constraint on α_C must be found. The following three possible scenarios are possible:

(i) set the angle of attack to a predefined value, say $\alpha_C = \alpha_{C_0}$;
(ii) find the angle of attack that minimizes the thrust required to drive the vehicle along the desired trimming trajectory Υ_C;
(iii) set the bow control surface to zero at trim, and find the angle of attack α_C as a function of the desired trimming trajectory Υ_C.

Due to the difficulty in measuring the angle of attack, the first two options will be hard to use in practice. The third, however, is easily enforced by introducing a 'washout' during the control design phase to ensure zero bow control plane deflection at trimming, leading to the steady state constraint

$$\delta_{bc} = 0$$

3.2.4. Constraint on roll angle

Due to physical vehicle characteristics (metacentric height versus torque generated by the control surfaces) the roll angle will be kept always small and the vehicle will be trimmed at $\phi_C = 0$.

It is important to remark that for some types of vehicles (e.g. fully actuated remotely operated vehicles) there is considerably more freedom in selecting the desired vehicle attitude along trimming trajectories. In this case, additional parameters can be included as scheduling variables or additional constraints have to be imposed to compute the trimming vectors.

4. GENERALIZED ERROR DYNAMICS

The gain scheduling methodology proposed for integrated design of a guidance and control system for the non-linear system $\mathcal{P}$ described by Equations (21) involves obtaining linear models for $\mathcal{P}$ along trimming trajectories in the set $\mathcal{E}$. These models will necessarily be time varying in the co-ordinates used to write (21). It turns out, however, that appropriate error co-ordinate systems exist where the linearization of the plant $\mathcal{P}$ along any trajectory $\Upsilon_C \in \mathcal{E}$ is time invariant. One of these co-ordinate systems is discussed next.

Before proceeding, consider Figure 2 where $\mathcal{R}$ represents the co-ordinate transformation from body fixed co-ordinate system $\{B\}$ to inertial frame $\{I\}$ and $\{C\}$ corresponds to the body axis co-ordinate system at trimming. The matrices $\mathcal{R}_E$ and $\mathcal{R}_C$ represent the co-ordinate transformations from $\{B\}$ to $\{C\}$ and from $\{C\}$ to $\{I\}$, respectively. Using these definitions, it is clear that

$$\mathcal{R}_E = \mathcal{R}_C^{-1}\mathcal{R} \tag{30}$$

Let $\mathbf{p}_C, \boldsymbol{\lambda}_C \in \mathcal{E}$ be given. Define the non-linear transformation [7]

$$\mathrm{NLT} = \begin{cases} \mathbf{v}_E = \mathbf{v} - \mathbf{v}_C \\ \boldsymbol{\omega}_E = \boldsymbol{\omega} - \boldsymbol{\omega}_C \\ \mathbf{p}_E = \mathcal{R}^{-1}(\mathbf{p} - \mathbf{p}_C) \\ \boldsymbol{\lambda}_E = \arg(\mathcal{R}_E) \end{cases} \tag{31}$$

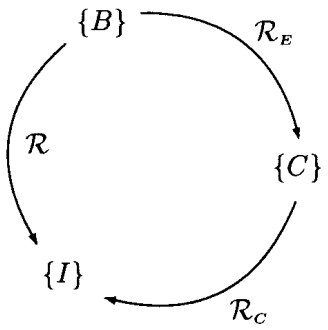

Figure 2. Relationship among co-ordinate systems.

with

$$\arg(\mathcal{R}_E) = \begin{cases} \theta_E = \text{atan2}\left(-r_{31}, \sqrt{r_{11}^2 + r_{21}^2}\right) \\ \psi_E = \text{atan2}(r_{21}/\cos(\theta_E), r_{11}/\cos(\theta_E)) \\ \phi_E = \text{atan2}(r_{32}/\cos(\theta_E), r_{33}/\cos(\theta_E)) \end{cases}$$

where atan2(.,.) is the two argument arc tangent function, and r_{ij} represents the ijth element of matrix $\mathcal{R}_E$ [16]. Further let $\mathbf{u}_E = \mathbf{u} - \mathbf{u}_C$. The non-linear co-ordinate transformation (31) can be interpreted as the generalized error vector between the vehicle state and the trajectory in $\mathcal{E}$.

It will now be shown that in the new *error* co-ordinate system the linearization of the rigid body dynamics given by (21) along any arbitrary trajectory in $\mathcal{E}$ is time invariant. To obtain the linearization of the rigid body dynamics in the new co-ordinate system, the time derivatives of the new error variables defined in (31) must be computed first. It is obvious that

$$\frac{\mathrm{d}}{\mathrm{d}t}\mathbf{v}_E = \frac{\mathrm{d}}{\mathrm{d}t}\mathbf{v} - \frac{\mathrm{d}}{\mathrm{d}t}\mathbf{v}_C$$

and

$$\frac{\mathrm{d}}{\mathrm{d}t}\boldsymbol{\omega}_E = \frac{\mathrm{d}}{\mathrm{d}t}\boldsymbol{\omega} - \frac{\mathrm{d}}{\mathrm{d}t}\boldsymbol{\omega}_C$$

From the definition of $\mathbf{p}_E$,

$$\mathbf{p}_C = \mathbf{p} - \mathcal{R}\mathbf{p}_E$$

and

$$\frac{\mathrm{d}}{\mathrm{d}t}\mathbf{p}_C = \frac{\mathrm{d}}{\mathrm{d}t}\mathbf{p} - \mathcal{R}\mathcal{S}(\boldsymbol{\omega})\mathbf{p}_E - \mathcal{R}\frac{\mathrm{d}}{\mathrm{d}t}\mathbf{p}_E$$

where $\mathcal{S}(\boldsymbol{\omega})$ is the skew symmetric matrix defined by $\mathcal{S}(\boldsymbol{\omega}) = \boldsymbol{\omega}\times$ (see the appendix). Since $(\mathrm{d}/\mathrm{d}t)\mathbf{p} = \mathcal{R}\mathbf{v}$ and $(\mathrm{d}/\mathrm{d}t)\mathbf{p}_C = \mathcal{R}_C\mathbf{v}_C$ it follows that

$$\mathcal{R}_C\mathbf{v}_C = \mathcal{R}\mathbf{v} - \mathcal{R}\mathcal{S}(\boldsymbol{\omega})\mathbf{p}_E - \mathcal{R}\frac{\mathrm{d}}{\mathrm{d}t}\mathbf{p}_E \tag{32}$$

Pre-multiplying both sides of Equation (32) by $\mathcal{R}^{-1}$ and using $\mathcal{R}_E^{-1} = \mathcal{R}^{-1}\mathcal{R}_C$ Equation (32) yields

$$\frac{\mathrm{d}}{\mathrm{d}t}\mathbf{p}_E = \mathbf{v} - \mathcal{R}_E^{-1}\mathbf{v}_C - \mathcal{S}(\boldsymbol{\omega})\mathbf{p}_E$$

The time derivative of $\boldsymbol{\lambda}_E$ is computed using the well-known relationship (see Reference [16] for further details)

$$\frac{\mathrm{d}}{\mathrm{d}t}\boldsymbol{\lambda}_E = \mathcal{Q}_E[\boldsymbol{\omega} - \mathcal{R}_E^{-1}\boldsymbol{\omega}_C]$$

where $\mathcal{Q}_E = Q(\boldsymbol{\lambda}_E)$.

Since for any trimming trajectory $\Upsilon_C \in \mathcal{E}$ the vectors $\mathbf{v}_C$ and $\boldsymbol{\omega}_C$ are constant, the above equations can be written as

$$\begin{cases} \dfrac{\mathrm{d}}{\mathrm{d}t}\mathbf{v}_E = \dfrac{\mathrm{d}}{\mathrm{d}t}\mathbf{v} \\ \dfrac{\mathrm{d}}{\mathrm{d}t}\boldsymbol{\omega}_E = \dfrac{\mathrm{d}}{\mathrm{d}t}\boldsymbol{\omega} \\ \dfrac{\mathrm{d}}{\mathrm{d}t}\mathbf{p}_E = \mathbf{v} - \mathcal{R}_E^{-1}\mathbf{v}_C - \mathcal{S}(\boldsymbol{\omega})\mathbf{p}_E \\ \dfrac{\mathrm{d}}{\mathrm{d}t}\boldsymbol{\lambda}_E = \mathcal{Q}_E[\boldsymbol{\omega} - \mathcal{R}_E^{-1}\boldsymbol{\omega}_C] \end{cases} \tag{33}$$

Finally, using Equation (21) one obtains

$$\mathcal{P}_E = \begin{cases} \dfrac{\mathrm{d}}{\mathrm{d}t}\mathbf{v}_E = \mathcal{F}_{\mathbf{v}}(\mathbf{v},\boldsymbol{\omega}) + \mathcal{F}_{\mathbf{v}}^{\boldsymbol{\lambda}}(\boldsymbol{\lambda}) + \mathcal{B}_{\mathbf{v}}(\mathbf{v},\boldsymbol{\omega})\mathcal{H}(\mathbf{v},\mathbf{u}) \\ \dfrac{\mathrm{d}}{\mathrm{d}t}\boldsymbol{\omega}_E = \mathcal{F}_{\boldsymbol{\omega}}(\mathbf{v},\boldsymbol{\omega}) + \mathcal{F}_{\boldsymbol{\omega}}^{\boldsymbol{\lambda}}(\boldsymbol{\lambda}) + \mathcal{B}_{\boldsymbol{\omega}}(\mathbf{v},\boldsymbol{\omega})\mathcal{H}(\mathbf{v},\mathbf{u}) \\ \dfrac{\mathrm{d}}{\mathrm{d}t}\mathbf{p}_E = \mathbf{v} - \mathcal{R}_E^{-1}\mathbf{v}_C - \mathcal{S}(\boldsymbol{\omega})\mathbf{p}_E \\ \dfrac{\mathrm{d}}{\mathrm{d}t}\boldsymbol{\lambda}_E = \mathcal{Q}_E[\boldsymbol{\omega} - \mathcal{R}_E^{-1}\boldsymbol{\omega}_C] \end{cases} \tag{34}$$

which corresponds to the non-linear plant depicted in Figure 3. The main result of this section is stated next.

Theorem 4.1

Let $\Upsilon_C \in \mathcal{E}$ be an arbitrary trimming trajectory of a rigid body $\bar{\mathcal{R}}$, and let $\boldsymbol{\eta}_C$ be the corresponding parametrizing vector. Consider the generalized error dynamics $\mathcal{P}_E$ in (34) that result from applying the non-linear transformation (31) to the rigid body equations (21). Then, the linearization of $\mathcal{P}_E$ about the zero solution (or equivalently, the linearization of the rigid body dynamics about Υ_C, expressed in the new co-ordinates of (31)) is time invariant, with

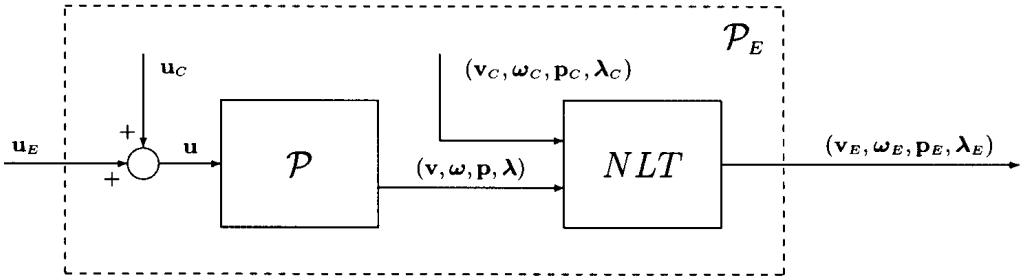

Figure 3. Non-linear plant representation.

realization

$$\mathcal{P}_L(\boldsymbol{\eta}_C) = \begin{cases} \dfrac{\mathrm{d}}{\mathrm{d}t}\delta\mathbf{v}_E = A_{\mathbf{v}}^{\mathbf{v}}\delta\mathbf{v}_E + A_{\mathbf{v}}^{\boldsymbol{\omega}}\delta\boldsymbol{\omega}_E + A_{\mathbf{v}}^{\boldsymbol{\lambda}}\delta\boldsymbol{\lambda}_E + B_{\mathbf{v}}\delta\mathbf{u} \\ \dfrac{\mathrm{d}}{\mathrm{d}t}\delta\boldsymbol{\omega}_E = A_{\boldsymbol{\omega}}^{\mathbf{v}}\delta\mathbf{v}_E + A_{\boldsymbol{\omega}}^{\boldsymbol{\omega}}\delta\boldsymbol{\omega}_E + A_{\boldsymbol{\omega}}^{\boldsymbol{\lambda}}\delta\boldsymbol{\lambda}_E + B_{\boldsymbol{\omega}}\delta\mathbf{u} \\ \dfrac{\mathrm{d}}{\mathrm{d}t}\delta\mathbf{p}_E = \delta\mathbf{v}_E - \mathcal{S}(\boldsymbol{\omega}_C)\delta\mathbf{p}_E - \mathcal{S}(\mathbf{v}_C)\delta\boldsymbol{\lambda}_E \\ \dfrac{\mathrm{d}}{\mathrm{d}t}\delta\boldsymbol{\lambda}_E = \delta\boldsymbol{\omega}_E - \mathcal{S}(\boldsymbol{\omega}_C)\delta\boldsymbol{\lambda}_E \end{cases} \tag{35}$$

where

$$\begin{aligned} &A_{\mathbf{v}}^{\mathbf{v}} \equiv \frac{\partial}{\partial\mathbf{v}}[\mathcal{F}_{\mathbf{v}}(.) + \mathcal{B}_{\mathbf{v}}(.)\mathcal{H}(.)], \quad A_{\mathbf{v}}^{\boldsymbol{\omega}} \equiv \frac{\partial}{\partial\boldsymbol{\omega}}[\mathcal{F}_{\mathbf{v}}(.) + \mathcal{B}_{\mathbf{v}}(.)\mathcal{H}(.)], \\ &B_{\mathbf{v}} \equiv \frac{\partial}{\partial\mathbf{u}}[\mathcal{B}_{\mathbf{v}}(.)\mathcal{H}(.)], \\ &A_{\boldsymbol{\omega}}^{\mathbf{v}} \equiv \frac{\partial}{\partial\mathbf{v}}[\mathcal{F}_{\boldsymbol{\omega}}(.) + \mathcal{B}_{\boldsymbol{\omega}}(.)\mathcal{H}(.)], \quad A_{\boldsymbol{\omega}}^{\boldsymbol{\omega}} \equiv \frac{\partial}{\partial\boldsymbol{\omega}}[\mathcal{F}_{\boldsymbol{\omega}}(.) + \mathcal{B}_{\boldsymbol{\omega}}(.)\mathcal{H}(.)], \\ &B_{\boldsymbol{\omega}} \equiv \frac{\partial}{\partial\mathbf{u}}[\mathcal{B}_{\boldsymbol{\omega}}(.)\mathcal{H}(.)] \end{aligned} \tag{36}$$

with

$$A_{\mathbf{v}}^{\boldsymbol{\lambda}} \equiv \frac{\partial}{\partial\boldsymbol{\lambda}}\mathcal{F}_{\mathbf{v}}^{\boldsymbol{\lambda}}(.) = M_{\mathbf{v}}\mathcal{S}(\mathcal{R}_C^{-1}\mathbf{g}), \quad A_{\boldsymbol{\omega}}^{\boldsymbol{\lambda}} \equiv \frac{\partial}{\partial\boldsymbol{\lambda}}\mathcal{F}_{\boldsymbol{\omega}}^{\boldsymbol{\lambda}}(.) = M_{\boldsymbol{\omega}}\mathcal{S}(\mathcal{R}_C^{-1}\mathbf{g})$$

and all partial derivatives are computed at trimming values.

For simplicity the system output equation is not written explicitly in realization (35) since its form is problem dependent and will be clear from the context.

Remark
Trim invariance of the error dynamics is a result of resolving the tracking errors in a co-ordinate system attached to the body. As such, similar results can be obtained for any rigid body tracking trimming trajectories.

Proof

To prove Theorem 4.1 Equations (34) can be linearized to derive the linearization $\mathcal{P}_L(\boldsymbol{\eta}_C)$ of $\mathcal{P}_E$ about the zero solution (with a certain abuse of notation, we will often refer to $\mathcal{P}_L(\boldsymbol{\eta}_C)$ as the linearization of the rigid body Equations (21) about Υ_C).

Start with the dynamic equations. From the definition of $\mathbf{v}_E$ and $\boldsymbol{\omega}_E$ it follows that

$$\begin{aligned} \delta\mathbf{v}_E &= \delta\mathbf{v} \\ \delta\boldsymbol{\omega}_E &= \delta\boldsymbol{\omega} \end{aligned} \tag{37}$$

and therefore

$$\begin{aligned} \frac{\mathrm{d}}{\mathrm{d}t}\delta\mathbf{v}_E &= \frac{\mathrm{d}}{\mathrm{d}t}\delta\mathbf{v}l \\ \frac{\mathrm{d}}{\mathrm{d}t}\delta\boldsymbol{\omega}_E &= \frac{\mathrm{d}}{\mathrm{d}t}\delta\boldsymbol{\omega} \end{aligned} \tag{38}$$

Computing the linearization of (34) and applying Equations (38) and Identity 10.1 from the appendix, gives the time invariant equations

$$\begin{aligned} \frac{\mathrm{d}}{\mathrm{d}t}\delta\mathbf{v}_E &= A_{\mathbf{v}}^{\mathbf{v}}\delta\mathbf{v}_E + A_{\mathbf{v}}^{\boldsymbol{\omega}}\delta\boldsymbol{\omega}_E + A_{\mathbf{v}}^{\boldsymbol{\lambda}}\delta\boldsymbol{\lambda}_E + \mathcal{B}_{\mathbf{v}}\delta\mathbf{u} \\ \frac{\mathrm{d}}{\mathrm{d}t}\delta\boldsymbol{\omega}_E &= A_{\boldsymbol{\omega}}^{\mathbf{v}}\delta\mathbf{v}_E + A_{\boldsymbol{\omega}}^{\boldsymbol{\omega}}\delta\boldsymbol{\omega}_E + A_{\boldsymbol{\omega}}^{\boldsymbol{\lambda}}\delta\boldsymbol{\lambda}_E + \mathcal{B}_{\boldsymbol{\omega}}\delta\mathbf{u} \end{aligned} \tag{39}$$

Consider now the kinematic equations. Recall that if $\mathbf{w}$ is a vector of $\mathbb{R}^3$, then the following relationships hold (see the appendix):

$$\frac{\mathrm{d}}{\mathrm{d}\boldsymbol{\lambda}}(\mathcal{R}\mathbf{w}) = -\mathcal{R}\mathcal{S}(\mathbf{w})\mathcal{Q}^{-1}(\boldsymbol{\lambda}) \quad \text{and} \quad \frac{\mathrm{d}}{\mathrm{d}\boldsymbol{\lambda}}(\mathcal{R}^{-1}\mathbf{w}) = \mathcal{S}(\mathcal{R}^{-1}\mathbf{w})\mathcal{Q}^{-1}(\boldsymbol{\lambda}) \tag{40}$$

To compute the linearization of $(\mathrm{d}/\mathrm{d}t)\mathbf{p}_E$, observe that $\boldsymbol{\lambda}_E = 0$ and $\mathcal{R}_E = I$ along trimming trajectories $\Upsilon_C \in \mathcal{E}$. Using the above relationship it is easy to obtain

$$\frac{\partial}{\partial\boldsymbol{\lambda}_E}(\mathcal{R}_E^{-1}\mathbf{v}_C)\bigg|_{\boldsymbol{\lambda}_E=0} = \mathcal{S}(\mathcal{R}_E\mathbf{v}_C)\mathcal{Q}_E^{-1}|_{\boldsymbol{\lambda}_E=0} = \mathcal{S}(\mathbf{v}_C)$$

and therefore

$$\frac{\mathrm{d}}{\mathrm{d}t}\delta\mathbf{p}_E = \delta\mathbf{v} - \mathcal{S}(\mathbf{v}_C)\delta\boldsymbol{\lambda}_E - \mathcal{S}(\boldsymbol{\omega}_C)\delta\mathbf{p}_E \tag{41}$$

To compute the linearization of $(\mathrm{d}/\mathrm{d}t)\boldsymbol{\lambda}_E$, observe first that

$$\frac{\mathrm{d}}{\mathrm{d}t}\boldsymbol{\lambda}_E = \mathcal{Q}_E\boldsymbol{\omega}_E + \mathcal{Q}_E(I - \mathcal{R}_E^{-1})\boldsymbol{\omega}_C$$

Let $\mathbf{y} = (I - \mathcal{R}_E^{-1})\boldsymbol{\omega}_C$. Then,

$$\frac{\mathrm{d}}{\mathrm{d}t}\delta\boldsymbol{\lambda}_E = \mathcal{Q}_E|_{\boldsymbol{\lambda}_E=0}\delta\boldsymbol{\omega}_E + \frac{\partial}{\partial\boldsymbol{\lambda}_E}(\mathcal{Q}_E)\mathbf{y}\bigg|_{\boldsymbol{\lambda}_E=0}\delta\boldsymbol{\lambda}_E - \mathcal{Q}_E\frac{\partial}{\partial\boldsymbol{\lambda}_E}(\mathcal{R}_E^{-1}\boldsymbol{\omega}_C)\bigg|_{\boldsymbol{\lambda}_E=0}\delta\boldsymbol{\lambda}_E$$

Since along a trimming trajectory the vector $\mathbf{y}$ equals 0, using the right-hand side identity of (40) one obtains

$$\frac{\mathrm{d}}{\mathrm{d}t}\delta\boldsymbol{\lambda}_E = \delta\boldsymbol{\omega}_E - \mathcal{S}(\boldsymbol{\omega}_C)\delta\boldsymbol{\lambda}_E$$

Thus, the linearized model admits the time invariant realization (35) thereby completing the proof of Theorem 4.1. □

Equation (35) can be used to define a family of linear plants $\mathcal{P}_L$ associated with the set $\mathcal{E}$. Let $\Upsilon_C \in \mathcal{E}$ and define

$$\delta\mathbf{x}_{\mathrm{dyn}_E} = \begin{bmatrix} \delta\mathbf{v}_E \\ \delta\boldsymbol{\omega}_E \end{bmatrix}, \quad \delta\mathbf{x}_{\mathrm{kin}_E} = \begin{bmatrix} \delta\mathbf{p}_E \\ \delta\boldsymbol{\lambda}_E \end{bmatrix}$$

Then

$$\mathcal{P}_L(\boldsymbol{\eta}_C) \coloneqq \begin{cases} \dfrac{\mathrm{d}}{\mathrm{d}t}\delta\mathbf{x}_{\mathrm{dyn}_E} = A_d^d(\boldsymbol{\eta}_C)\delta\mathbf{x}_{\mathrm{dyn}_E} + A_k^d(\boldsymbol{\eta}_C)\delta\mathbf{x}_{\mathrm{kin}_E} + B(\boldsymbol{\eta}_C)\delta\mathbf{u} \\ \dfrac{\mathrm{d}}{\mathrm{d}t}\delta\mathbf{x}_{\mathrm{kin}_E} = \delta\mathbf{x}_{\mathrm{dyn}_E} + A_k^k(\boldsymbol{\eta}_C)\delta\mathbf{x}_{\mathrm{kin}_E} \end{cases}$$

where

$$A_d^d = \begin{bmatrix} A_{\mathbf{v}}^{\mathbf{v}} & A_{\mathbf{v}}^{\boldsymbol{\omega}} \\ A_{\boldsymbol{\omega}}^{\mathbf{v}} & A_{\boldsymbol{\omega}}^{\boldsymbol{\omega}} \end{bmatrix}, \quad A_k^d = \begin{bmatrix} 0 & A_{\mathbf{v}}^{\boldsymbol{\lambda}} \\ 0 & A_{\boldsymbol{\omega}}^{\boldsymbol{\lambda}} \end{bmatrix}, \quad A_k^k = \begin{bmatrix} -\mathcal{S}(\boldsymbol{\omega}_C) & -\mathcal{S}(\mathbf{v}_C) \\ 0 & -\mathcal{S}(\boldsymbol{\omega}_C) \end{bmatrix}, \quad B = \begin{bmatrix} B_{\mathbf{v}} \\ B_{\boldsymbol{\omega}} \end{bmatrix}$$

Formally,

$$\mathcal{P}_L \coloneqq \{\mathcal{P}_L(\boldsymbol{\eta}_C),\ \boldsymbol{\eta}_C = [\mathbf{V}_{\tau_c}, \dot{\psi}_C, \gamma_C]^{\mathrm{T}}\}$$

The utility of the family of linear plants $\mathcal{P}_L$ as well as the perturbed kinematic error $\delta\mathbf{x}_{\mathrm{kin}_E}$ will become evident in the next section.

5. TRAJECTORY TRACKING CONTROLLER IMPLEMENTATION PROBLEM

In the previous section it was shown that linearization of the rigid body dynamics about any trimming trajectory in $\mathcal{E}$ results in a time invariant plant $\mathcal{P}_L(\boldsymbol{\eta}_C)$. Therefore, associated with the set $\mathcal{E}$ there is a family of linear plants $\mathcal{P}_L$ which can be used to synthesize a gain scheduled tracking controller $\mathcal{C}$ designed to operate about all the trajectories $\Upsilon_C \in \mathcal{E}$. Following common practice, this involves designing a family of linear controllers for a *finite* number of linear plants $\mathcal{P}_L(\boldsymbol{\eta}_C)$ in $\mathcal{P}_L$, and then interpolating between these controllers to achieve adequate performance for all the linearized plants in $\mathcal{P}_L$. During real time operation, the controller parameters are updated as functions of the time-varying gain scheduling variable $\boldsymbol{\eta}$. This is illustrated in the feedback system represented in Figure 4, where $\mathcal{P}$ is the rigid body model dynamic model to be controlled. The controller $\mathcal{C}(\boldsymbol{\eta})$, that operates on the measured variables $\mathbf{y}$ to produce the control input $\mathbf{u}$, is scheduled on the parameter $\boldsymbol{\eta} = [\mathbf{V}_\tau, \dot{\psi}, \gamma]^{\mathrm{T}}$ measured in real time. In the figure,

$$\Upsilon_R = [\mathbf{p}_R^{\mathrm{T}}, \boldsymbol{\lambda}_R^{\mathrm{T}}]^{\mathrm{T}}$$

is the input vector to be tracked by the corresponding variables in $\mathbf{x}_{\mathrm{kin}}$. Notice that this captures the general case where desired values are specified for both the vehicle's position and attitude.

In what follows, the study will be restricted to the idealized case where the description of each controller for each plant in $\mathcal{P}_L$ is available [18]. Therefore, it is assumed that the first design step

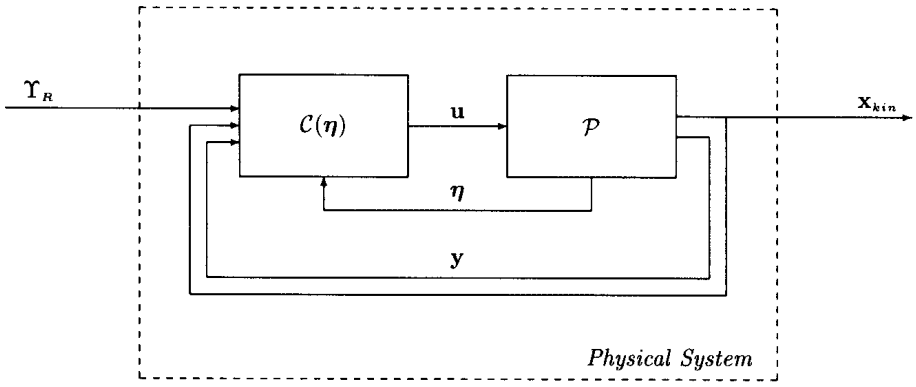

Figure 4. Feedback interconnection of non-linear plant $\mathcal{P}$ and controller $C(\boldsymbol{\eta})$.

produces the set

$$\mathcal{C}_L := \{\mathcal{C}_L(\boldsymbol{\eta}_C), \boldsymbol{\eta}_C = [\mathbf{V}_{\tau_c}, \dot{\psi}_C, \gamma_C]^{\mathrm{T}}\}$$

where $\mathcal{C}_L$ is a controller designed to operate about $\boldsymbol{\eta}_C$.

5.1. The output feedback case

Figure 5 depicts the general structure of a linear tracking controller for a plant $\mathcal{C}_L(\boldsymbol{\eta}_C)$. The dynamic block $\mathcal{K}(\boldsymbol{\eta}_C)$ has realization

$$\mathcal{K}(\boldsymbol{\eta}_C) = \left[\begin{array}{c|ccc} A_{c_1}(\boldsymbol{\eta}_C) & B_{c_1}(\boldsymbol{\eta}_C) & B_{c_2}(\boldsymbol{\eta}_C) & B_{c_3}(\boldsymbol{\eta}_C) \\ \hline C_{c_1}(\boldsymbol{\eta}_C) & D_{c_1}(\boldsymbol{\eta}_C) & D_{c_2}(\boldsymbol{\eta}_C) & D_{c_3}(\boldsymbol{\eta}_C) \end{array}\right]$$

corresponding to the linear controller implementation

$$\mathcal{C}_L(\boldsymbol{\eta}_C) = \begin{cases} \dfrac{\mathrm{d}}{\mathrm{d}t}\delta\mathbf{x}_{c_1} = A_{c_1}(\boldsymbol{\eta}_C)\delta\mathbf{x}_{c_1} + B_{c_1}(\boldsymbol{\eta}_C)C_d\delta\mathbf{x}_{\mathrm{dyn}_E} + B_{c_2}(\boldsymbol{\eta}_C)(\delta\mathbf{x}_{\mathrm{kin}_E} - \boldsymbol{\zeta}) \\ \qquad\qquad + B_{c_3}(\boldsymbol{\eta}_C)\delta\mathbf{x}_{c_2} \\ \dfrac{\mathrm{d}}{\mathrm{d}t}\delta\mathbf{x}_{c_2} = S_1(\delta\mathbf{x}_{\mathrm{kin}_E} - \boldsymbol{\zeta}) + S_2\delta\mathbf{u} \\ \delta\mathbf{u} = C_{c_1}(\boldsymbol{\eta}_C)\delta\mathbf{x}_{c_1} + D_{c_1}(\boldsymbol{\eta}_C)C_d\delta\mathbf{x}_{\mathrm{dyn}_E} + D_{c_2}(\boldsymbol{\eta}_C)(\delta\mathbf{x}_{\mathrm{kin}_E} - \boldsymbol{\zeta}) \\ \qquad + D_{c_3}(\boldsymbol{\eta}_C)\delta\mathbf{x}_{c_2} \end{cases} \tag{42}$$

where $[\delta\mathbf{x}_{c_1}^{\mathrm{T}}, \delta\mathbf{x}_{c_2}^{\mathrm{T}}]^{\mathrm{T}} \in \mathbb{R}^{n_c+m}$ is the controller state, $\delta\mathbf{u} \in \mathbb{R}^m$ is the input to the plant, and matrix C_d selects the components of $\mathbf{x}_{\mathrm{dyn}_E}$ that are accessible for measurement. The fictitious input $\boldsymbol{\zeta}$ is introduced to assess tracking performance of the linearized closed loop system. Matrices $S_1 \in \mathbb{R}^{m\times p}$ and $S_2 \in \mathbb{R}^{m\times m}$ select q and $m-q$ components of vectors $\delta\mathbf{x}_{\mathrm{kin}_E}$ and $\delta\mathbf{u}$, respectively, that must be driven to zero along trimming trajectories. For example, in the case of an AUV it may

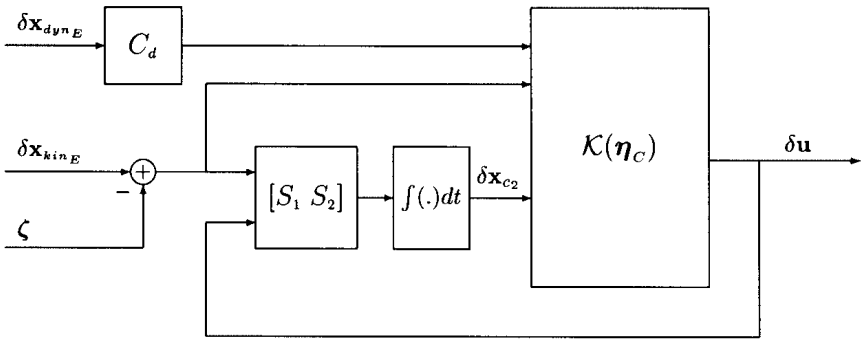

Figure 5. Linear controller $\mathcal{C}_L(\boldsymbol{\eta}_C)$.

be required to drive the tracking error of certain kinematic variables as well as the bow plane deflection to zero while leaving the other kinematic variables and inputs unconstrained. As is common in control system design, this is done by including integrators that are driven by the constrained variables. The total number of integrators equals the number of inputs to the plant. Thus,

$$S_1 = \begin{bmatrix} X_1 \\ 0 \end{bmatrix}, \quad X_1 \in \mathbb{R}^{q \times p}; \quad X_1 \text{ full row rank}$$

and

$$S_2 = \begin{bmatrix} 0 \\ X_2 \end{bmatrix}, \quad X_2 \in \mathbb{R}^{(m-q) \times m}; \quad X_2 \text{ full row rank}$$

It is assumed that the parameters of the controller are C^1 functions of $\boldsymbol{\eta}_C$.

The structure of the controller $\mathcal{C}_L$ is represented in Figure 5 and has the following important feature. Suppose the closed loop system consisting of Equations (35) and (42) is asymptotically stable. Then the controller $\mathcal{C}_L(\boldsymbol{\eta}_C)$ will ensure zero steady-state error to a step input for the variables in $S_1(\delta \mathbf{x}_{\text{kin}_E} - \boldsymbol{\zeta})$ as well as zero steady-state actuation for the actuators in $S_2 \delta \mathbf{u}$. This is achieved by integrating $S_1(\delta \mathbf{x}_{\text{kin}_E} - \boldsymbol{\zeta}) + S_2 \delta \mathbf{u}$. This structure is typical of tracking controllers, since they are designed to drive errors between step changes in reference commands and the corresponding plant outputs to zero at steady state. Notice that the block $\mathcal{K}(\boldsymbol{\eta}_C)$ (see Figure 5) may itself contain additional integrators.

In the framework of gain scheduled control the family of linear controllers $\mathcal{C}_L$ must be implemented on the non-linear plant $\mathcal{P}$ defined in Section 4. This issue is usually referred to as the controller implementation problem. See Reference [10] where this problem was addressed for a specific class of non-linear plants and tracking controllers. Motivated by the analysis presented in Reference [10] let $\Upsilon_C \in \mathcal{E}$ be a trimming trajectory and $\boldsymbol{\eta}_C$ the corresponding trimming parameter. Further let

$$\mathcal{T}(\mathcal{P}_L(\boldsymbol{\eta}_C), \mathcal{C}_L(\boldsymbol{\eta}_C)) : \boldsymbol{\zeta} \to \delta \mathbf{x}_{\text{kin}_E}$$

be the closed loop linear operator that results from connecting $\mathcal{C}_L(\boldsymbol{\eta}_C)$ to $\mathcal{P}_L(\boldsymbol{\eta}_C)$, and denote by $T(\mathcal{P}_L(\boldsymbol{\eta}_C), \mathcal{C}_L(\boldsymbol{\eta}_C))(s)$ the corresponding matrix transfer function. Let

$$\mathcal{T}(\mathcal{P}, \mathcal{C})(\boldsymbol{\eta}_C) : \ \Upsilon_R \to \mathbf{x}_{\text{kin}}$$

be the non-linear closed loop system that consists of $\mathcal{C}$ and $\mathcal{P}$, and let

$$\tilde{\mathcal{T}}_l(\mathcal{P},\mathcal{C})(\boldsymbol{\eta}_C)$$

denote the operator that results from its linearization about $\Upsilon_C \in \mathcal{E}$.

For performance assessment, it is important to find out how the resulting control system reacts in response to small perturbations in the commands Υ_R about the nominal trajectory Υ_C. Define the operator

$$\mathcal{T}_l(\mathcal{P},\mathcal{C})(\boldsymbol{\eta}_C) = L^{-1}(\boldsymbol{\lambda}_C)\tilde{\mathcal{T}}_l(\mathcal{P},\mathcal{C})(\boldsymbol{\eta}_C)L(\boldsymbol{\lambda}_C)$$

where the time varying transformation $L(\boldsymbol{\lambda}_C)$ is given by

$$L(\boldsymbol{\lambda}_C) = \begin{bmatrix} \mathcal{R}_C & 0 \\ 0 & \mathcal{Q}_C \end{bmatrix}$$

It will be shown that $\mathcal{T}_l(\mathcal{P},\mathcal{C})(\boldsymbol{\eta}_C)$ is time invariant and can be viewed as the 'trajectory compensated' linearization of the non-linear closed loop system about Υ_C. Denote by $\mathcal{T}_l(\mathcal{P},\mathcal{C})(\boldsymbol{\eta}_C)(s)$ the corresponding matrix transfer function. With this notation, the rigid body trajectory tracking controller implementation problem addressed in this paper can be stated as follows:

5.1.1. Trajectory tracking controller implementation problem
Find a gain scheduled controller $C(\boldsymbol{\eta})$ such that for each $\Upsilon_C \in \mathcal{E}$

(i) the feedback systems $\mathcal{T}_l(\mathcal{P},\mathcal{C})(\boldsymbol{\eta}_C)$ and $\mathcal{T}(\mathcal{P}_L(\boldsymbol{\eta}_C),\mathcal{C}_L(\boldsymbol{\eta}_C))$ have the same closed loop eigenvalues;
(ii) the closed loop transfer functions $\mathcal{T}_l((\mathcal{P},\mathcal{C})(\boldsymbol{\eta}_C))(s)$ and $\mathcal{T}(\mathcal{P}_L(\boldsymbol{\eta}_C),\mathcal{C}_L(\boldsymbol{\eta}_C))(s)$ are equal.

Notice the basic requisites set forth in the trajectory tracking controller implementation problem that both internal (eigenvalue placement) and external (input output behaviour) properties be preserved.

A complete solution to the trajectory tracking controller implementation problem is provided below. Given the set $\mathcal{C}_L$ of linear controllers for the set $\mathcal{P}_L$ of linearized plant models, consider the following structure as an implementation proposal for the gain scheduled controller $\mathcal{C}(\boldsymbol{\eta})$ (see Figure 6)

$$\mathcal{C}(\boldsymbol{\eta}) \coloneqq \begin{cases} \tilde{\mathbf{x}}_{\mathrm{kin}_E} = [\mathcal{R}^{-1}[\mathbf{p}-\mathbf{p}_R]^{\mathrm{T}}, \arg(\tilde{\mathcal{R}}_E)^{\mathrm{T}}]^{\mathrm{T}} \\ \dfrac{\mathrm{d}}{\mathrm{d}t}\mathbf{x}_{c_1} = A_{c_1}(\boldsymbol{\eta})\mathbf{x}_{c_1} + B_{c_1}(\boldsymbol{\eta})C_d\dfrac{\mathrm{d}}{\mathrm{d}t}\mathbf{x}_{\mathrm{dyn}} + B_{c_2}(\boldsymbol{\eta})\dfrac{\mathrm{d}}{\mathrm{d}t}\tilde{\mathbf{x}}_{\mathrm{kin}_E} \\ \qquad\qquad + B_{c_3}(\boldsymbol{\eta})[S_2\mathbf{u} + S_1\tilde{\mathbf{x}}_{\mathrm{kin}_E}] \\ \dfrac{\mathrm{d}}{\mathrm{d}t}\mathbf{x}_{c_2} = C_{c_1}(\boldsymbol{\eta})\mathbf{x}_{c_1} + D_{c_1}(\boldsymbol{\eta})C_d\dfrac{\mathrm{d}}{\mathrm{d}t}\mathbf{x}_{\mathrm{dyn}} + D_{c_2}(\boldsymbol{\eta})\dfrac{\mathrm{d}}{\mathrm{d}t}\tilde{\mathbf{x}}_{\mathrm{kin}_E} \\ \qquad\qquad + D_{c_3}(\boldsymbol{\eta})[S_2\mathbf{u} + S_1\tilde{\mathbf{x}}_{\mathrm{kin}_E}] \\ \mathbf{u} = \mathbf{x}_{c_2} \end{cases} \tag{43}$$

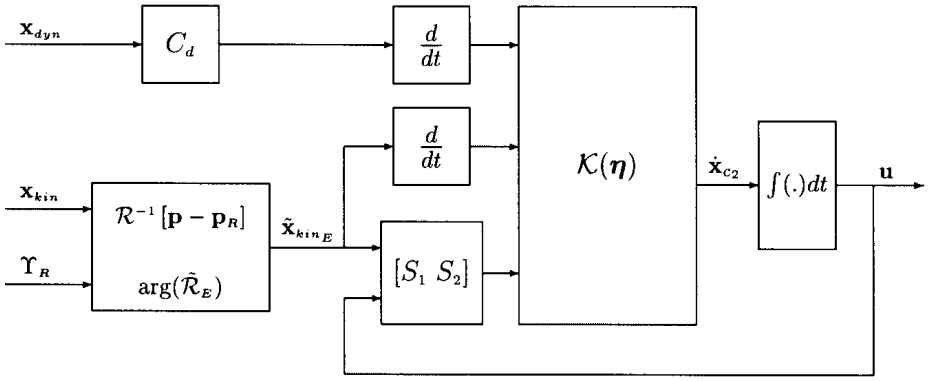

Figure 6. Non-linear controller $\mathcal{C}(\boldsymbol{\eta})$.

where matrix $\tilde{\mathcal{R}}_E = \mathcal{R}(\boldsymbol{\lambda}_R)^{\mathrm{T}}\mathcal{R}$ represents the co-ordinate transformation from $\{B\}$ to command frame, parameterized locally by vector $\boldsymbol{\lambda}_R$. Notice in Figures 5 and 6 that the structure of the gain scheduled controller is easily obtained from that of the linear controllers.

Consider the following assumptions:

A1. $\dim(\mathbf{x}_{c_2}) = \dim(\mathbf{u}) = \dim(S_1\tilde{\mathbf{x}}_{\mathrm{kin}_E} + S_2\mathbf{u})$

A2. The matrix

$$\begin{bmatrix} sI - A_{c_1}(\boldsymbol{\eta}) & B_{c_3}(\boldsymbol{\eta}) \\ -C_{c_1}(\boldsymbol{\eta}) & D_{c_3}(\boldsymbol{\eta}) \end{bmatrix}$$

has full rank at $s = 0$ for each $\Upsilon_C \in \mathcal{E}$.

A3. The matrix pair (A_{c_1}, C_{c_1}) is observable.

Assumption A1 implies that the number of integrators is equal to the number of control inputs. This is necessary if the controller is to provide independent control of the signals $S_1\tilde{\mathbf{x}}_{\mathrm{kin}_E} + S_2\mathbf{u}$ using the control inputs $\mathbf{u}$. Assumption A2 implies that the realization $(A_{c_1}, B_{c_3}, C_{c_1}, D_{c_3})$ has no transmission zeroes at the origin. Finally, assumption A3 guarantees that the state $\mathbf{x}_{c_1}$ is zero along trajectories in $\mathcal{E}$.

The main result of this section is stated next.

Theorem 5.1

Given $\mathcal{C}_L$, suppose assumptions A1, A2, and A3 hold. Then the gain scheduled controller $\mathcal{C}$ given by Equations (43) solves the trajectory tracking controller implementation problem.

It follows from the theorem that the eigenvalues of the linearization along each trajectory in $\mathcal{E}$ are preserved. Furthermore, the input–output behaviour of the linearized operators is preserved in a well-defined sense. The reader is referred to Reference [10] for a complete discussion on approximations to continuous and discrete time controller implementation methodology that avoid using pure differentiation and that can be directly applied to the closed loop trajectory tracking controller implementation, if needed.

Proof

In the proof the controller matrices D_{c_1} and D_{c_2} will be set to zero. This does not change the results but simplifies the algebra considerably. In addition, in some of the expressions the explicit dependence of the controller parameters on $\boldsymbol{\eta}_C$ will be dropped.

Let $\boldsymbol{\eta}_C$ be given, and consider the feedback interconnection of the linearized plant $\mathcal{P}_L(\boldsymbol{\eta}_C)$ and the corresponding linear controller $\mathcal{C}_L(\boldsymbol{\eta}_C)$. The state matrix $F(\boldsymbol{\eta}_C)$ of the feedback system can be written as

$$F(\boldsymbol{\eta}_C) := \begin{bmatrix} A_d^d & A_k^d & BC_{c_1} & BD_{c_3} \\ I_{6\times 6} & A_k^k & 0 & 0 \\ B_{c_1}C_d & B_{c_2} & A_{c_1} & B_{c_3} \\ 0 & S_1 & S_2C_{c_1} & S_2D_{c_3} \end{bmatrix} \tag{44}$$

where for notational simplicity the explicit dependence of the matrices $A_{(.)}, B_{(.)}$, and $C_{(.)}$ on $\boldsymbol{\eta}_C$ was omitted.

The feedback interconnection of the plant $\mathcal{P}$ and the controller $\mathcal{C}(\boldsymbol{\eta})$ shown in Figure 6 is now linearized about the equilibrium 'condition' corresponding to the trimming trajectory determined by $\boldsymbol{\eta}_C$. Notice that at equilibrium $\Upsilon_R = \Upsilon_C$ and $\mathbf{x}_{\text{dyn}} = \mathbf{x}_{\text{dyn}_C} = 0$. However, $\mathbf{x}_{\text{kin}_E}$ may be different from zero since not all angular kinematic variables are required to achieve perfect tracking.

First, the states $\mathbf{x}_{c_{1_0}}$ and $\mathbf{x}_{c_{2_0}}$ and the output $\mathbf{u}_C$ of the controller corresponding to this equilibrium condition are determined. Consider the set of algebraic equations

$$\begin{aligned} 0 = {} & A_{c_1}(\boldsymbol{\eta}_C)\mathbf{x}_{c_1} + B_{c_1}(\boldsymbol{\eta}_C)C_d \frac{\mathrm{d}}{\mathrm{d}t}\mathbf{x}_{\text{dyn}} + B_{c_2}(\boldsymbol{\eta}_C)\frac{\mathrm{d}}{\mathrm{d}t}\tilde{\mathbf{x}}_{\text{kin}_E} \\ & + B_{c_3}(\boldsymbol{\eta}_C)[S_2\mathbf{u}_C + S_1\tilde{\mathbf{x}}_{\text{kin}_E}] \end{aligned} \tag{45}$$

$$0 = C_{c_1}(\boldsymbol{\eta}_C)\mathbf{x}_{c_1} + D_{c_3}(\boldsymbol{\eta}_C)[S_2\mathbf{u}_C + S_1\tilde{\mathbf{x}}_{\text{kin}_E}] \tag{46}$$

$$\mathbf{u} = \mathbf{x}_{c_2} \tag{47}$$

Since $\mathbf{x}_{\text{dyn}}$ and $\tilde{\mathbf{x}}_{\text{kin}_E}$ are constant along trimming trajectories it follows that $(\mathrm{d}/\mathrm{d}t)\mathbf{x}_{\text{dyn}} = 0$ and $(\mathrm{d}/\mathrm{d}t)\tilde{\mathbf{x}}_{\text{kin}_E} = (\mathrm{d}/\mathrm{d}t)\mathbf{x}_{\text{kin}_E} = 0$. Therefore, Equations (45) and (46) can be written in matrix form as

$$\begin{bmatrix} A_{c_1}(\boldsymbol{\eta}_C) & B_{c_3}(\boldsymbol{\eta}_C) \\ C_{c_1}(\boldsymbol{\eta}_C) & D_{c_3}(\boldsymbol{\eta}_C) \end{bmatrix} \begin{bmatrix} \mathbf{x}_{c_{1_0}} \\ S_2\mathbf{u}_C + S_1\tilde{\mathbf{x}}_{\text{kin}_E} \end{bmatrix} = 0$$

Assumptions A1–A2 imply that the matrix

$$\begin{bmatrix} A_{c_1}(\boldsymbol{\eta}_C) & B_{c_3}(\boldsymbol{\eta}_C) \\ C_{c_1}(\boldsymbol{\eta}_C) & D_{c_3}(\boldsymbol{\eta}_C) \end{bmatrix} \tag{48}$$

is square and invertible for each $\boldsymbol{\eta}_C$. It then follows from the assumptions and Equation (47) that

$$S_2\mathbf{u}_C + S_1\tilde{\mathbf{x}}_{\text{kin}_E} = 0$$
$$\mathbf{x}_{c_{1_0}} = 0$$
$$\mathbf{x}_{c_{2_0}} = \mathbf{u}_C$$

It is now necessary to compute the state matrix for the linearized feedback interconnection of $\mathcal{P}$ and $\mathcal{C}(\boldsymbol{\eta})$. Consider Figure 6. Notice that the non-linear controller can be equivalently viewed as a dynamic system $\bar{\mathcal{C}}(\boldsymbol{\eta})$ with inputs $C_d\mathbf{x}_{\text{dyn}}$ and $\mathbf{x}_{\text{kin}_E} = \tilde{\mathbf{x}}_{\text{kin}_E}$ and output $\mathbf{u}$, where the second equality comes from the fact that $\Upsilon_R = \Upsilon_C$. A simple reasoning shows that the above mentioned linearization is obtained by combining the linearization $\bar{\mathcal{C}}_L(\boldsymbol{\eta})$ of $\bar{\mathcal{C}}(\boldsymbol{\eta})$ (about the equilibrium point defined by $\mathbf{x}_{c_{1_0}} = 0$, $\mathbf{x}_{c_{2_0}} = \mathbf{u}_C$, $(\mathrm{d}/\mathrm{d}t)\tilde{\mathbf{x}}_{\text{kin}_E} = 0$, $(\mathrm{d}/\mathrm{d}t)\mathbf{x}_{\text{dyn}_C} = 0$ and $S_1\tilde{\mathbf{x}}_{\text{kin}_E} + S_2\mathbf{u}_C = 0$) with the linearized system $\mathcal{P}_L$ in (35).

To compute the linearization of $\tilde{\mathcal{C}}(\boldsymbol{\eta})$ define vectors

$$\bar{f}(\boldsymbol{\eta}) = A_{c_1}\mathbf{x}_{c_1} + B_{c_1}C_d\frac{\mathrm{d}}{\mathrm{d}t}\mathbf{x}_{\text{dyn}_E} + B_{c_2}\frac{\mathrm{d}}{\mathrm{d}t}\tilde{\mathbf{x}}_{\text{kin}_E} + B_{c_3}[S_2\mathbf{u} + S_1\tilde{\mathbf{x}}_{\text{kin}_E}]$$
$$\bar{g}(\boldsymbol{\eta}) = A_{c_1}\mathbf{x}_{c_1} + D_{c_3}[S_2\mathbf{u} + S_1\tilde{\mathbf{x}}_{\text{kin}_E}]$$

where the dependence of matrices $A_{(.)}, B_{(.)}, C_{(.)}$, and $D_{(.)}$, on the equilibrium trajectory was omitted. Then

$$\frac{\mathrm{d}}{\mathrm{d}t}\delta\mathbf{x}_{c_1} = \frac{\partial}{\partial\mathbf{u}}\bar{f}(\boldsymbol{\eta})\Big|_{\boldsymbol{\eta}=\boldsymbol{\eta}_C}\delta\mathbf{u} + \frac{\partial}{\partial\mathbf{x}_{\text{dyn}_E}}\bar{f}(\boldsymbol{\eta})\Big|_{\boldsymbol{\eta}=\boldsymbol{\eta}_C}\delta\mathbf{x}_{\text{dyn}_E} + \frac{\partial}{\partial\tilde{\mathbf{x}}_{\text{kin}_E}}\bar{f}(\boldsymbol{\eta})\Big|_{\boldsymbol{\eta}=\boldsymbol{\eta}_C}\delta\tilde{\mathbf{x}}_{\text{kin}_E} + \frac{\partial}{\partial\mathbf{x}_{c_1}}\bar{f}(\boldsymbol{\eta})\Big|_{\boldsymbol{\eta}=\boldsymbol{\eta}_C}\delta\mathbf{x}_{c_1}$$

$$\frac{\mathrm{d}}{\mathrm{d}t}\delta\mathbf{x}_{c_2} = \frac{\partial}{\partial\mathbf{u}}\bar{g}(\boldsymbol{\eta})\Big|_{\boldsymbol{\eta}=\boldsymbol{\eta}_C}\delta\mathbf{u} + \frac{\partial}{\partial\mathbf{x}_{\text{dyn}_E}}\bar{g}(\boldsymbol{\eta})\Big|_{\boldsymbol{\eta}=\boldsymbol{\eta}_C}\delta\mathbf{x}_{\text{dyn}_E} + \frac{\partial}{\partial\tilde{\mathbf{x}}_{\text{kin}_E}}\bar{g}(\boldsymbol{\eta})\Big|_{\boldsymbol{\eta}=\boldsymbol{\eta}_C}\delta\mathbf{x}_{\text{kin}_E} + \frac{\partial}{\partial\mathbf{x}_{c_1}}\bar{g}(\boldsymbol{\eta})\Big|_{\boldsymbol{\eta}=\boldsymbol{\eta}_C}\delta\mathbf{x}_{c_1}$$

$$\delta\mathbf{u} = \delta\mathbf{x}_{c_2}$$

where $(.)|_{\boldsymbol{\eta}=\boldsymbol{\eta}_C}$ means that expression inside brackets is evaluated along the equilibrium trajectory determined by $\boldsymbol{\eta}_C$. Note that since $\mathbf{x}_{c_{1_0}} = 0$,

$$\frac{\partial}{\partial\mathbf{x}_{\text{dyn}_E}}[A_{c_1}(\boldsymbol{\eta})x_{c_1}]\Big|_{\boldsymbol{\eta}=\boldsymbol{\eta}_C} = 0 \tag{49}$$

Similar results can be obtained for $(\partial/\partial\mathbf{x}_{\text{kin}_E})[A_{c_1}(\boldsymbol{\eta}_C)\mathbf{x}_{c_1}]|_{\boldsymbol{\eta}=\boldsymbol{\eta}_C}$, $(\partial/\partial\mathbf{u})[B_{c_1}(\boldsymbol{\eta}_C)(\mathrm{d}/\mathrm{d}t)\mathbf{x}_{\text{dyn}_E}]|_{\boldsymbol{\eta}=\boldsymbol{\eta}_C}$, etc. Therefore, the linearization of the controller has the form

$$\frac{\mathrm{d}}{\mathrm{d}t}\delta\mathbf{x}_{c_1} = A_{c_1}(\boldsymbol{\eta}_C)\delta\mathbf{x}_{c_1} + B_{c_1}(\boldsymbol{\eta}_C)C_d\frac{\mathrm{d}}{\mathrm{d}t}\delta\mathbf{x}_{\text{dyn}} + B_{c_2}(\boldsymbol{\eta}_C)\frac{\mathrm{d}}{\mathrm{d}t}\delta\tilde{\mathbf{x}}_{\text{kin}_E} + B_{c_3}(\boldsymbol{\eta}_C)[S_2\delta\mathbf{u} + S_1\delta\tilde{\mathbf{x}}_{\text{kin}_E}]$$

$$\frac{\mathrm{d}}{\mathrm{d}t}\delta\mathbf{x}_{c_2} = C_{c_1}(\boldsymbol{\eta}_C)\delta\mathbf{x}_{c_1} + D_{c_3}(\boldsymbol{\eta}_C)[S_2\delta\mathbf{u} + S_1\delta\tilde{\mathbf{x}}_{\mathrm{kin}_E}]$$

$$\delta\mathbf{u} = \delta\mathbf{x}_{c_2} \tag{50}$$

It is easy to verify that the state matrix $M(\boldsymbol{\eta}_C)$ of $\mathcal{T}_l(\mathcal{P},\mathcal{C})(\boldsymbol{\eta}_C)$ is

$$M(\boldsymbol{\eta}_C) \coloneqq \begin{bmatrix} A_d^d & A_k^d & 0 & B \\ I_{6\times 6} & A_k^k & 0 & 0 \\ B_{c_1}C_dA_d^d + B_{c_2} & B_{c_1}C_dA_k^d + B_{c_2}A_k^k + B_{c_3}S_1 & A_{c_1} & B_{c_1}C_dB + B_{c_3}S_2 \\ 0 & D_{c_3}S_1 & C_{c_1} & D_{c_3}S_2 \end{bmatrix} \tag{51}$$

where again the explicit dependence of the elements of matrix $M(\boldsymbol{\eta}_C)$ on the operating point has been omitted. To complete the proof of the first part of the theorem, it must be shown that there exists a non-singular matrix P such that $F = PMP^{-1}$. Earlier in the proof, it was shown that the matrix

$$\begin{bmatrix} A_{c_1} & B_{c_3} \\ C_{c_1} & D_{c_3} \end{bmatrix} \tag{52}$$

is invertible. Let

$$\begin{bmatrix} X & Y \\ Z & W \end{bmatrix} \coloneqq \begin{bmatrix} A_{c_1} & B_{c_3} \\ C_{c_1} & D_{c_3} \end{bmatrix}^{-1} \tag{53}$$

and set

$$P(\boldsymbol{\eta}_C) \coloneqq \begin{bmatrix} I_{6\times 6} & 0 & 0 & 0 \\ 0 & I_{6\times 6} & 0 & 0 \\ -XB_{c_1}C_d & -XB_{c_2} & X & Y \\ -ZB_{c_1}C_d & -ZB_{c_2} & Z & W \end{bmatrix}$$

Routine algebra shows that

$$P^{-1}(\boldsymbol{\eta}_C) \coloneqq \begin{bmatrix} I_{6\times 6} & 0 & 0 & 0 \\ 0 & I_{6\times 6} & 0 & 0 \\ B_{c_1}C_d & B_{c_2} & A_{c_1} & B_{c_3} \\ 0 & 0 & C_{c_1} & D_{c_3} \end{bmatrix}$$

and that

$$P(\boldsymbol{\eta}_C)M(\boldsymbol{\eta}_C) = \begin{bmatrix} A_d^d & A_k^d & 0 & B \\ I_{6\times 6} & A_k^k & 0 & 0 \\ 0 & 0 & I_{6\times 6} & 0 \\ 0 & S_1 & 0 & S_2 \end{bmatrix}$$

which leads to the conclusion that $F(\boldsymbol{\eta}_C) = P(\boldsymbol{\eta}_C)M(\boldsymbol{\eta}_C)P^{-1}(\boldsymbol{\eta}_C)$. Thus, $F(\boldsymbol{\eta}_C)$ and $M(\boldsymbol{\eta}_C)$ have the same eigenvalues. Note that this result is independent of matrices S_1 and S_2.

In order to show that

$$T_l((\mathcal{P},\mathcal{C})(\boldsymbol{\eta}_C))(s) = T(\mathcal{P}_L(\boldsymbol{\eta}_C),\mathcal{C}_L(\boldsymbol{\eta}_C))(s)$$

it is first proved that the transfer function of the linear controller (42) with input $\delta\mathbf{x}_{\text{kin}_E} - \boldsymbol{\zeta}$ and output $\delta\mathbf{u}$ equals the transfer function of the nonlinear controller linearization (50) from $\delta\tilde{\mathbf{x}}_{\text{kin}_E}$ to $\delta\mathbf{u}$. The first is given by

$$\begin{aligned}\mathbf{U}(s) = C_{c_1}(sI - A_{c_1})^{-1}\Big[&B_{c_1}C_d\mathbf{X}_{\text{dyn}}(s) + B_{c_2}(\mathbf{X}_{\text{kin}_E}(s) - \mathbf{Z}(s))\\ &+ B_{c_3}\frac{I}{s}[S_1(\mathbf{X}_{\text{kin}_E}(s) - \mathbf{Z}(s)) + S_2\mathbf{U}(s)]\Big]\\ &+ D_{c_3}\frac{I}{s}[S_1(\mathbf{X}_{\text{kin}_E}(s) - \mathbf{Z}(s)) + S_2\mathbf{U}(s)]\end{aligned}$$

while the latter can be written as

$$\begin{aligned}\mathbf{U}(s) = \frac{1}{s}C_{c_1}(sI - A_{c_1})^{-1}[&sB_{c_1}C_d\mathbf{X}_{\text{dyn}}(s) + sB_{c_2}\tilde{\mathbf{X}}_{\text{kin}_E}(s)\\ &+ B_{c_3}[S_1\tilde{\mathbf{X}}_{\text{kin}_E}(s) + S_2\mathbf{U}(s)]]\\ &+ D_{c_3}\frac{I}{s}[S_1(\tilde{\mathbf{X}}_{\text{kin}_E}(s) + S_2\mathbf{U}(s)]\end{aligned}$$

where $\mathbf{U}(s), \mathbf{X}_{\text{kin}_E}(s)$, $\tilde{\mathbf{X}}_{\text{kin}_E}(s)$, $\mathbf{Z}(s)$, and $\mathbf{X}_{\text{dyn}}(s)$ denote the Laplace transforms of $\delta\mathbf{u}$, $\delta\mathbf{x}_{\text{kin}_E}$, $\delta\tilde{\mathbf{x}}_{\text{kin}_E}, \boldsymbol{\zeta}$ and $\delta\mathbf{x}_{\text{dyn}_E}$, respectively. Simple computations show that the above transfer functions are equal.

Linearizing $\tilde{\mathbf{x}}_{\text{kin}_E} = [\tilde{\mathbf{p}}_E^{\mathrm{T}}, \tilde{\boldsymbol{\lambda}}_E^{\mathrm{T}}]^{\mathrm{T}}$ about equilibrium trajectories $\Upsilon_C \in \mathcal{E}$ gives

$$\begin{aligned}\delta\tilde{\mathbf{p}}_E = &\frac{\partial}{\partial\boldsymbol{\lambda}}\mathcal{R}^{-1}[\mathbf{p} - \mathbf{p}_R]\Big|_{\substack{\boldsymbol{\lambda}=\boldsymbol{\lambda}_C\\ \mathbf{p}=\mathbf{p}_C\\ \mathbf{p}_R=\mathbf{p}_C}}\delta\boldsymbol{\lambda} + \frac{\partial}{\partial\mathbf{p}}\mathcal{R}^{-1}[\mathbf{p} - \mathbf{p}_R]\Big|_{\substack{\boldsymbol{\lambda}=\boldsymbol{\lambda}_C\\ \mathbf{p}=\mathbf{p}_C\\ \mathbf{p}_R=\mathbf{p}_C}}\delta\mathbf{p}\\ &+ \frac{\partial}{\partial\mathbf{p}_C}\mathcal{R}^{-1}[\mathbf{p} - \mathbf{p}_R]\Big|_{\substack{\boldsymbol{\lambda}=\boldsymbol{\lambda}_C\\ \mathbf{p}=\mathbf{p}_C\\ \mathbf{p}_R=\mathbf{p}_C}}\delta\tilde{\mathbf{p}}\end{aligned}$$

which can be written as

$$\delta\tilde{\mathbf{p}}_E = \mathcal{R}_C^{-1}[\delta\mathbf{p} - \delta\tilde{\mathbf{p}}] \tag{54}$$

Furthermore,

$$\delta\tilde{\boldsymbol{\lambda}}_E = \frac{\partial}{\partial\boldsymbol{\lambda}}\arg(\tilde{\mathcal{R}}_E)\Big|_{\substack{\boldsymbol{\lambda}=\boldsymbol{\lambda}_C\\ \boldsymbol{\lambda}_R=\boldsymbol{\lambda}_C}}\delta\boldsymbol{\lambda} + \frac{\partial}{\partial\tilde{\boldsymbol{\lambda}}}\arg(\tilde{\mathcal{R}}_E)\Big|_{\substack{\boldsymbol{\lambda}=\boldsymbol{\lambda}_C\\ \boldsymbol{\lambda}_R=\boldsymbol{\lambda}_C}}\delta\tilde{\boldsymbol{\lambda}}$$

which, after some algebraic manipulations can be expressed as

$$\delta\tilde{\boldsymbol{\lambda}}_E = \mathcal{Q}_C^{-1}[\delta\boldsymbol{\lambda} - \delta\tilde{\boldsymbol{\lambda}}] \tag{55}$$

Now, using Equations (54) and (55), the linearization of $\tilde{\mathbf{x}}_{\text{kin}_E}$ about the equilibrium trajectories can be written as

$$\delta\tilde{\mathbf{x}}_{\text{kin}_E} = L(\boldsymbol{\lambda}_C)^{-1}(\delta\mathbf{x}_{\text{kin}} - \delta\tilde{\Upsilon}) \tag{56}$$

Setting $\delta\tilde{\Upsilon} = L(\lambda_C)\zeta$, and using the fact that $\delta\mathbf{x}_{\mathrm{kin}_E} = L(\lambda_C)^{-1}\delta\mathbf{x}_{\mathrm{kin}}$ the theorem follows immediately from the definition of the operator

$$\mathcal{T}_1(\mathcal{P},\mathcal{C})(\eta_C) = L^{-1}(\lambda_C)\tilde{\mathcal{T}}_l(\mathcal{P},\mathcal{C})(\eta_C)L(\lambda_C) \qquad \square$$

It is worth emphasizing the following important properties of the controller $\mathcal{C}$:

1. The result in Theorem 5.1 holds for all trimming trajectories $\Upsilon_C \in \mathcal{E}$.
2. The structure of the controller $\mathcal{C}(\eta)$ is easily obtained from that of the linear controllers $\mathcal{C}_L(\eta_C)$.
3. All closed loop transfer functions of the local linearization are preserved. Therefore, at the level of local linear analysis the controller does not introduce any additional noise amplification despite the presence of a differentiation operator.
4. At equilibrium, $\mathbf{x}_{c_{2_0}} = \mathbf{u}_C$ and $\mathbf{x}_{c_{1_0}} = 0$. Therefore, controller initialization is simple and the plant input trimming value is naturally provided by the integrator block with state $\mathbf{x}_{c_2}$.
5. The integrators $\mathbf{x}_{c_2}$ are directly at the input of the plant thus making the implementation of anti-windup schemes straightforward [19]. This becomes necessary in applications where the input $\mathbf{u}$ is hard limited due to actuator saturations, for example, in the case of underwater vehicles and airplanes where the actuator saturation is present either in thruster actuation or control surface deflections.
6. Given a vehicle trimming strategy, the inputs to the controller $\mathbf{x}_{\mathrm{kin}_C}$ can be computed directly from the vector η_C and the initial conditions of the trajectory to be tracked.
7. The trim values $\mathbf{x}_{\mathrm{dyn}_C}$ and $\mathbf{u}_C$ are not required in the controller implementation.
8. Along the trajectories $\Upsilon_C \in \mathcal{E}$ the controller guarantees that the error vector $S_1\tilde{\mathbf{x}}_{\mathrm{kin}_E}$ is zero. This is in sharp contrast to standard LOS guidance schemes.
9. For most applications only the time derivative of the vehicle angular velocity $\boldsymbol{\omega}$ must be computed directly. The other derivatives are, in general, available from on-board sensors. In fact, instead of computing the time derivative of $\mathbf{x}_{\mathrm{kin}_E}$ the relationship

$$\frac{\mathrm{d}}{\mathrm{d}t}\mathbf{x}_{\mathrm{kin}_E} = \begin{bmatrix} \dfrac{\mathrm{d}}{\mathrm{d}t}\mathcal{R}^{-1}[\mathbf{p}-\mathbf{p}_R] \\ \dfrac{\mathrm{d}}{\mathrm{d}t}\arg(\tilde{\mathcal{R}}_E) \end{bmatrix} = \begin{bmatrix} -\mathcal{S}(\boldsymbol{\omega})\mathcal{R}^{-1}[\mathbf{p}-\mathbf{p}_R] + \mathcal{R}^{-1}[\frac{\mathrm{d}}{\mathrm{d}t}\mathbf{p} - \dfrac{\mathrm{d}}{\mathrm{d}t}\mathbf{p}_R] \\ \mathcal{Q}_E[\boldsymbol{\omega} - \mathcal{R}_E^{-1}[\boldsymbol{\omega}-\boldsymbol{\omega}_R]] \end{bmatrix}$$

can be used, where $\boldsymbol{\omega}_R$ is the reference angular velocity and $(\mathrm{d}/\mathrm{d}t)\mathbf{p}$ is the inertial velocity of the vehicle. In most cases, the latter is available from on-board Doppler effect sensors (e.g. Doppler radar and Doppler sonar for aircraft and underwater vehicles, respectively). Similarly, the time derivative of the body velocity $(\mathrm{d}/\mathrm{d}t)\mathbf{v}$ can be obtained from

$$\frac{\mathrm{d}}{\mathrm{d}t}\mathbf{v} = \mathbf{a} - \mathcal{R}^{-1}\mathbf{g} - \mathcal{S}(\boldsymbol{\omega})\mathbf{v}$$

where $\mathbf{a}$ is the vector of specific accelerations measured by on-board accelerometers and $\mathbf{v} = \mathcal{R}^{-1}(\mathrm{d}/\mathrm{d}t)\mathbf{p}$.

5.2. *The state feedback case*

This section presents a solution to the trajectory tracking problem for the case where $\mathcal{K}(\eta_C)$ is obtained for the augmented plant using a state feedback synthesis technique. As in the previous

case, assume that the design step produces the set of linear controllers

$$\mathcal{C}_L := \begin{cases} \dfrac{\mathrm{d}}{\mathrm{d}t}\delta\mathbf{x}_c = S_1(\delta\mathbf{x}_{\mathrm{kin}_E} - \boldsymbol{\zeta}) + S_2\delta\mathbf{u} \\ \delta\mathbf{u} = K_1(\boldsymbol{\eta}_C)\delta\mathbf{x}_{\mathrm{dyn}} + K_2(\boldsymbol{\eta}_C)(\delta\mathbf{x}_{\mathrm{kin}_E} - \boldsymbol{\zeta}) + K_3(\boldsymbol{\eta}_C)\delta\mathbf{x}_c \end{cases} \tag{57}$$

with the structure displayed in Figure 5 where $C_d = I$ and $K_i(\boldsymbol{\eta}_C)$; $i = 1, 2, 3$ are matrices of appropriate dimensions. In the equations $\delta\mathbf{x}_c \in \mathbb{R}^m$ is the controller state and $\delta\mathbf{u} \in \mathbb{R}^m$ represents the input to the plant. The fictitious input $\boldsymbol{\zeta}$ is introduced to assess the tracking performance of the linearized closed loop system. Notice again the presence of a bank of integrators aimed at driving tracking errors to zero at steady state. As in the output feedback case, assume that the parameters of the controller are C^1 functions of $\boldsymbol{\eta}_C$.

Given the set C_L of linear controllers designed for the set $\mathcal{P}_L$ of linearized plant models, consider the following structure as an implementation scheme proposed for the gain scheduled controller $C(\boldsymbol{\eta})$ (see Figure 6 and set matrix $C_d = I$):

$$\mathcal{C}(\boldsymbol{\eta}) := \begin{cases} \tilde{\mathbf{x}}_{\mathrm{kin}_E} = [\mathcal{R}^{-1}[\mathbf{p} - \mathbf{p}_R]^{\mathrm{T}}, \arg(\tilde{\mathcal{R}}_E)^{\mathrm{T}}]^{\mathrm{T}} \\ \dfrac{\mathrm{d}}{\mathrm{d}t}\mathbf{x}_c = K_1(\boldsymbol{\eta}_C)\dfrac{\mathrm{d}}{\mathrm{d}t}\mathbf{x}_{\mathrm{dyn}} + K_2(\boldsymbol{\eta}_C)\dfrac{\mathrm{d}}{\mathrm{d}t}\tilde{\mathbf{x}}_{\mathrm{kin}_E} + K_3(\boldsymbol{\eta}_C)[S_2\mathbf{u} + S_1\tilde{\mathbf{x}}_{\mathrm{kin}_E}] \\ \mathbf{u} = \mathbf{x}_c \end{cases} \tag{58}$$

Once more notice that in Figures 5 and 6 the structure of the gain scheduled controller is easily obtained from that of the linear controllers. The following theorem presents the solution to the trajectory tracking implementation problem for the state feedback case. The proof is omitted.

Theorem 5.2
Given $\mathcal{C}_L$, assume that $\dim(\mathbf{x}_c) = \dim(\mathbf{u}) = \dim(S_1\tilde{\mathbf{x}}_{\mathrm{kin}_E} + S_2\mathbf{u})$ and that matrix $K_3(\boldsymbol{\eta}_C)$ is invertible. Then the gain scheduled controller $\mathcal{C}(\boldsymbol{\eta})$ given by Equations (58) solves the trajectory tracking controller implementation problem, i.e. for each $\Upsilon_C \in \mathcal{E}$ the following properties hold:

(i) The feedback systems $\mathcal{T}_l(\mathcal{P}, \mathcal{C})(\boldsymbol{\eta}_C)$ and $\mathcal{T}(\mathcal{P}_L(\boldsymbol{\eta}_C), \mathcal{C}_L(\boldsymbol{\eta}_C))$ have the same closed loop eigenvalues.
(ii) The closed loop matrix transfer functions $\mathcal{T}_l(\mathcal{P}, \mathcal{C})(\boldsymbol{\eta}_C)(s)$ and $\mathcal{T}(\mathcal{P}_L(\boldsymbol{\eta}_C), \mathcal{C}_L(\boldsymbol{\eta}_C))(s)$ are equal.

6. AN ALTERNATIVE CO-ORDINATE TRANSFORMATION

The non-linear transformation NLT in (31) played a key role in the development of the gain scheduled controller $\mathcal{C}(\boldsymbol{\eta})$. However, controller implementation is computationally intensive due to the need to determine $\arg(\mathcal{R}_E)$ in real time. This section shows how in the case under study a much simpler transformation can be used that still yields useful results. The new transformation is obtained by redefining $\boldsymbol{\lambda}_E$ as $\boldsymbol{\lambda}_E = \mathcal{Q}^{-1}[\boldsymbol{\lambda} - \boldsymbol{\lambda}_C]$, where $\mathcal{Q}^{-1} = \mathcal{Q}^{-1}(\boldsymbol{\lambda})$ is a constant matrix about each trimming trajectory $\Upsilon_C \in \mathcal{E}$ and $\mathcal{Q}$ satisfies $(\mathrm{d}/\mathrm{d}t)\boldsymbol{\lambda} = \mathcal{Q}\boldsymbol{\omega}$. In this case, the non-linear

transformation (31) degenerates into

$$\begin{aligned} \mathbf{v}_E &= \mathbf{v} - \mathbf{v}_C \\ \boldsymbol{\omega}_E &= \boldsymbol{\omega} - \boldsymbol{\omega}_C \\ \mathbf{p}_E &= \mathcal{R}^{-1}[\mathbf{p} - \mathbf{p}_C] \\ \boldsymbol{\lambda}_E &= \mathcal{Q}^{-1}[\boldsymbol{\lambda} - \boldsymbol{\lambda}_C] \end{aligned} \tag{59}$$

Following Section 4 it must now be shown that the linearization of plant $\mathcal{P}$ in the error state space defined by Equation (59), computed along trimming trajectories $\Upsilon_C \in \mathcal{E}$, is time invariant.

In order to do this, the derivatives of $\mathbf{p}_E$ and $\boldsymbol{\lambda}_E$ about trimming trajectories Υ_C must first be computed. A result similar to that in Section 4 is obtained for $\mathbf{p}_E$, that is,

$$\frac{\mathrm{d}}{\mathrm{d}t}\mathbf{p}_E = \mathbf{v} - \mathcal{R}_E^{-1}\mathbf{v}_C - \mathcal{S}(\boldsymbol{\omega})\mathbf{p}_E \tag{60}$$

Computing the time derivative of $\boldsymbol{\lambda}_E = \mathcal{Q}^{-1}[\boldsymbol{\lambda} - \boldsymbol{\lambda}_C]$ gives

$$\frac{\mathrm{d}}{\mathrm{d}t}\boldsymbol{\lambda}_E = \mathcal{Q}^{-1}\left[\frac{\mathrm{d}}{\mathrm{d}t}\boldsymbol{\lambda} - \frac{\mathrm{d}}{\mathrm{d}t}\boldsymbol{\lambda}_C\right] + \frac{\mathrm{d}}{\mathrm{d}t}\mathcal{Q}^{-1}[\boldsymbol{\lambda} - \boldsymbol{\lambda}_C]$$

Using the fact that $(\mathrm{d}/\mathrm{d}t)\boldsymbol{\lambda} = \mathcal{Q}\boldsymbol{\omega}$ and $(\mathrm{d}/\mathrm{d}t)\boldsymbol{\lambda}_C = \mathcal{Q}_C\boldsymbol{\omega}_C$, one obtains

$$\frac{\mathrm{d}}{\mathrm{d}t}\boldsymbol{\lambda}_E = \mathcal{Q}^{-1}\mathcal{Q}\boldsymbol{\omega} - \mathcal{Q}^{-1}\mathcal{Q}_C\boldsymbol{\omega}_C + \frac{\mathrm{d}}{\mathrm{d}t}\mathcal{Q}^{-1}[\boldsymbol{\lambda} - \boldsymbol{\lambda}_C]$$

which can be simplified to give

$$\frac{\mathrm{d}}{\mathrm{d}t}\boldsymbol{\lambda}_E = \boldsymbol{\omega} - \mathcal{Q}^{-1}\mathcal{Q}_C\boldsymbol{\omega}_C + \frac{\mathrm{d}}{\mathrm{d}t}\mathcal{Q}^{-1}\mathcal{Q}\boldsymbol{\lambda}_E \tag{61}$$

Now, using Equations (59) and (60) and the fact that for trajectories $\Upsilon_C \in \mathcal{E}$ the vectors $\mathbf{v}_C$ and $\boldsymbol{\omega}_C$ are constant, the non-linear error model becomes

$$\mathcal{P}_E = \begin{cases} \dfrac{\mathrm{d}}{\mathrm{d}t}\mathbf{v}_E = \mathcal{F}_{\mathbf{v}}(\mathbf{v},\boldsymbol{\omega}) + \mathcal{F}_{\mathbf{v}}^{\boldsymbol{\lambda}}(\boldsymbol{\lambda}) + \mathcal{B}_{\mathbf{v}}(\mathbf{v},\boldsymbol{\omega})\mathcal{H}(\mathbf{v},\mathbf{u}) \\ \dfrac{\mathrm{d}}{\mathrm{d}t}\boldsymbol{\omega}_E = \mathcal{F}_{\boldsymbol{\omega}}(\mathbf{v},\boldsymbol{\omega}) + \mathcal{F}_{\boldsymbol{\omega}}^{\boldsymbol{\lambda}}(\boldsymbol{\lambda}) + \mathcal{B}_{\boldsymbol{\omega}}(\mathbf{v},\boldsymbol{\omega})\mathcal{H}(\mathbf{v},\mathbf{u}) \\ \dfrac{\mathrm{d}}{\mathrm{d}t}\mathbf{p}_E = \mathbf{v} - \mathcal{R}_E^{-1}\mathbf{v}_C - \mathcal{S}(\boldsymbol{\omega})\mathbf{p}_E \\ \dfrac{\mathrm{d}}{\mathrm{d}t}\boldsymbol{\lambda}_E = \boldsymbol{\omega} - \mathcal{Q}^{-1}\mathcal{Q}_C\boldsymbol{\omega}_C + \dfrac{\mathrm{d}}{\mathrm{d}t}\mathcal{Q}^{-1}\mathcal{Q}\boldsymbol{\lambda}_E \end{cases} \tag{62}$$

The linearization of this model about trimming trajectories gives a result similar to the one presented in Section 4; see the next theorem.

Theorem 6.1

Let $\Upsilon_C \in \mathcal{E}$ be an arbitrary trimming trajectory of a rigid body $\bar{\mathcal{R}}$, and let $\boldsymbol{\eta}_C$ be the corresponding parametrizing vector. Consider the generalized error dynamics $\mathcal{P}_E$ in (62) that result from applying the non-linear transformation (59) to the rigid body equations (21). Then,

the linearization of $\mathcal{P}_E$ about the zero solution is time invariant, with realization

$$\mathcal{P}_L(\boldsymbol{\eta}_C) = \begin{cases} \dfrac{\mathrm{d}}{\mathrm{d}t}\delta\mathbf{v}_E = A_{\mathbf{v}}^{\mathbf{v}}\delta\mathbf{v}_E + A_{\mathbf{v}}^{\boldsymbol{\omega}}\delta\boldsymbol{\omega}_E + A_{\mathbf{v}}^{\boldsymbol{\lambda}}\delta\boldsymbol{\lambda}_E + B_{\mathbf{v}}\delta\mathbf{u} \\ \dfrac{\mathrm{d}}{\mathrm{d}t}\delta\boldsymbol{\omega}_E = A_{\boldsymbol{\omega}}^{\mathbf{v}}\delta\mathbf{v}_E + A_{\boldsymbol{\omega}}^{\boldsymbol{\omega}}\delta\boldsymbol{\omega}_E + A_{\boldsymbol{\omega}}^{\boldsymbol{\lambda}}\delta\boldsymbol{\lambda}_E + B_{\boldsymbol{\omega}}\delta\mathbf{u} \\ \dfrac{\mathrm{d}}{\mathrm{d}t}\delta\mathbf{p}_E = \delta\mathbf{v}_E - \mathcal{S}(\boldsymbol{\omega}_C)\delta\mathbf{p}_E - \mathcal{S}(\mathbf{v}_C)\delta\boldsymbol{\lambda}_E \\ \dfrac{\mathrm{d}}{\mathrm{d}t}\delta\boldsymbol{\lambda}_E = \delta\boldsymbol{\omega}_E - \mathcal{S}(\boldsymbol{\omega}_C)\delta\boldsymbol{\lambda}_E \end{cases}$$

Proof

To prove Theorem 6.1 one needs to linearize equations (62) about the trajectories $\Upsilon_C \in \mathcal{E}$. The linearization of the first two equations of (62) gives

$$\begin{aligned} \frac{\mathrm{d}}{\mathrm{d}t}\delta\mathbf{v}_E &= A_{\mathbf{v}}^{\mathbf{v}}\delta\mathbf{v}_E + A_{\mathbf{v}}^{\boldsymbol{\omega}}\delta\boldsymbol{\omega}_E + A_{\mathbf{v}}^{\boldsymbol{\lambda}}\delta\boldsymbol{\lambda}_E + \mathcal{B}_{\mathbf{v}}\delta\mathbf{u} \\ \frac{\mathrm{d}}{\mathrm{d}t}\delta\boldsymbol{\omega}_E &= A_{\boldsymbol{\omega}}^{\mathbf{v}}\delta\mathbf{v}_E + A_{\boldsymbol{\omega}}^{\boldsymbol{\omega}}\delta\boldsymbol{\omega}_E + A_{\boldsymbol{\omega}}^{\boldsymbol{\lambda}}\delta\boldsymbol{\lambda}_E + \mathcal{B}_{\boldsymbol{\omega}}\delta\mathbf{u} \end{aligned} \tag{63}$$

as in Theorem 4.1. For the linearization of $(\mathrm{d}/\mathrm{d}t)\mathbf{p}_E$ one obtains

$$\begin{aligned} \frac{\mathrm{d}}{\mathrm{d}t}\delta\mathbf{p}_E = \delta\mathbf{v} &- \frac{\partial}{\partial\boldsymbol{\lambda}}[\mathcal{R}^{-1}(\mathcal{R}_C\mathbf{v}_C)]\frac{\partial\boldsymbol{\lambda}}{\partial\boldsymbol{\lambda}_E}\bigg|_{\boldsymbol{\eta}=\boldsymbol{\eta}_C}\delta\boldsymbol{\lambda}_E - \frac{\partial}{\partial\boldsymbol{\omega}}[\mathcal{S}(\boldsymbol{\omega})\mathbf{p}_E]\bigg|_{\boldsymbol{\eta}=\boldsymbol{\eta}_C}\delta\boldsymbol{\omega} \\ &- \frac{\partial}{\partial\mathbf{p}_E}[\mathcal{S}(\boldsymbol{\omega})\mathbf{p}_E]\bigg|_{\boldsymbol{\eta}=\boldsymbol{\eta}_C}\delta\mathbf{p}_E \end{aligned} \tag{64}$$

Evaluating the above equation along the trajectories in $\mathcal{E}$ and using Identity 10.1 from the appendix, results in

$$\frac{\mathrm{d}}{\mathrm{d}t}\delta\mathbf{p}_E = \delta\mathbf{v}_E - \mathcal{S}(\mathbf{v}_C)\mathcal{Q}^{-1}\frac{\partial\boldsymbol{\lambda}}{\partial\boldsymbol{\lambda}_E}\bigg|_{\boldsymbol{\eta}=\boldsymbol{\eta}_C}\delta\boldsymbol{\lambda}_E - \mathcal{S}(\boldsymbol{\omega}_C)\delta\mathbf{p}_E \tag{65}$$

Linearizing Equation (62) and using the result that along the trajectories $\Upsilon_C \in \mathcal{E}, (\mathrm{d}/\mathrm{d}t)\mathcal{Q}^{-1} = 0$, gives

$$\frac{\mathrm{d}}{\mathrm{d}t}\delta\boldsymbol{\lambda}_E = \delta\boldsymbol{\omega}_E - \frac{\partial}{\partial\boldsymbol{\lambda}}(\mathcal{Q}^{-1}\mathcal{Q}_C\boldsymbol{\omega}_C)\frac{\partial\boldsymbol{\lambda}}{\partial\boldsymbol{\lambda}_E}\bigg|_{\boldsymbol{\eta}=\boldsymbol{\eta}_C}\delta\boldsymbol{\lambda}_E \tag{66}$$

From the definition of $\boldsymbol{\lambda}_E$ it follows that

$$\frac{\partial\boldsymbol{\lambda}}{\partial\boldsymbol{\lambda}_E} = \mathcal{Q} \tag{67}$$

After some algebraic manipulations it is possible to show that along the equilibrium trajectories

$$\frac{\partial}{\partial\boldsymbol{\lambda}}(\mathcal{Q}^{-1}\mathcal{Q}_C\boldsymbol{\omega}_C)\mathcal{Q} = \mathcal{S}(\boldsymbol{\omega}_C) \tag{68}$$

which recovers the general case results for $\delta\mathbf{p}_E$ and $\delta\boldsymbol{\lambda}_E$

$$\begin{aligned}\frac{\mathrm{d}}{\mathrm{d}t}\delta\mathbf{p}_E &= \delta\mathbf{v}_E - \mathcal{S}(\boldsymbol{\omega}_C)\delta\mathbf{p}_E - \mathcal{S}(\mathbf{v}_C)\delta\boldsymbol{\lambda}_E \\ \frac{\mathrm{d}}{\mathrm{d}t}\delta\boldsymbol{\lambda}_E &= \delta\boldsymbol{\omega}_E - \mathcal{S}(\boldsymbol{\omega}_C)\delta\boldsymbol{\lambda}_E\end{aligned} \tag{69}$$

and completes the proof of the theorem. □

It is straightforward to show that the results for the rigid body trajectory tracking controller implementation problem presented in Section 5 can be extended to this case.

In a great number of applications, the only variables that must be accurately tracked are linear positions $\mathbf{p}_R$, the remaining kinematic variables being left free to accommodate extra trimming constraints. In such cases,

$$S_1 = \begin{bmatrix} I_{3\times 3} & 0 \\ 0 & 0 \end{bmatrix}$$

and the simplified implementation scheme presented in Figure 7 can be applied [14]. The most important simplification amounts to replacing the time derivative of $\tilde{\boldsymbol{\lambda}}_E = \mathcal{Q}^{-1}[\boldsymbol{\lambda} - \boldsymbol{\lambda}_R]$ by

$$\boldsymbol{\tau} = \left(\boldsymbol{\omega} - \mathcal{Q}^{-1}\frac{\mathrm{d}}{\mathrm{d}t}\boldsymbol{\lambda}_R\right)$$

where

$$\frac{\mathrm{d}}{\mathrm{d}t}\boldsymbol{\lambda}_R = [0, 0, \dot{\psi}_R]^{\mathrm{T}}$$

Notice in this case that the only external commands that must be supplied to the control system are the linear position $\mathbf{p}_R$ and the yaw rate $\dot{\psi}_R$. This fact can hardly be overemphasized, since the new controller implementation entirely avoids feedforwarding any extra trimming variables. The non-linear controller implementation is given by

$$\mathcal{C}(\boldsymbol{\eta}) \coloneqq \begin{cases} \tilde{\mathbf{p}}_E = \mathcal{R}^{-1}[\mathbf{p} - \mathbf{p}_R] \\ \dfrac{\mathrm{d}}{\mathrm{d}t}\mathbf{x}_{c_1} = A_{c_1}(\boldsymbol{\eta})\mathbf{x}_{c_1} + B_{c_1}(\boldsymbol{\eta})C_d\dfrac{\mathrm{d}}{\mathrm{d}t}\mathbf{x}_{\mathrm{dyn}} + B_{c_2}(\boldsymbol{\eta})[\dfrac{\mathrm{d}}{\mathrm{d}t}\tilde{\mathbf{p}}_E^{\mathrm{T}}, \boldsymbol{\tau}^{\mathrm{T}}]^{\mathrm{T}} \\ \qquad\qquad + B_{c_3}(\boldsymbol{\eta})[S_2\mathbf{u} + [\tilde{\mathbf{p}}_E^{\mathrm{T}}, 0^{\mathrm{T}}]^{\mathrm{T}}] \\ \dfrac{\mathrm{d}}{\mathrm{d}t}\mathbf{x}_{c_2} = C_{c_1}(\boldsymbol{\eta})\mathbf{x}_{c_1} + D_{c_1}(\boldsymbol{\eta})C_d\dfrac{\mathrm{d}}{\mathrm{d}t}\mathbf{x}_{\mathrm{dyn}} + D_{c_2}(\boldsymbol{\eta})[\dfrac{\mathrm{d}}{\mathrm{d}t}\tilde{\mathbf{p}}_E^{\mathrm{T}}, \boldsymbol{\tau}^{\mathrm{T}}]^{\mathrm{T}} \\ \qquad\qquad + D_{c_3}(\boldsymbol{\eta})[S_2\mathbf{u} + [\tilde{\mathbf{p}}_E^{\mathrm{T}}, 0^{\mathrm{T}}]^{\mathrm{T}}] \\ \mathbf{u} = \mathbf{x}_{c_2} \end{cases} \tag{70}$$

It can be shown that the results of Section 5 can be trivially particularized to this set-up.

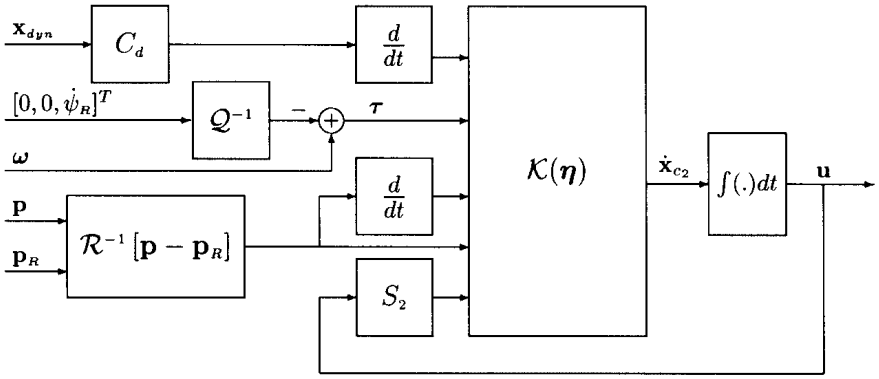

Figure 7. Simplified non-linear controller implementation.

7. EXAMPLE: AUV GUIDANCE/CONTROL SYSTEM DESIGN

This section illustrates the application of the methodology described before to the design of a gain scheduled trajectory tracking controller for the Infante AUV depicted in Figure 8. In what follows, a summary is given of the work required at each of the design steps that lead to the development of a controller for the vehicle that is scheduled on yaw rate $\dot{\psi}$ and flight path angle γ, that is, on the gain scheduling variable $\boldsymbol{\eta} = [\mathbf{V}_\tau, \dot{\psi}, \gamma]^{\mathrm{T}}$. The desired total velocity is kept constant. For the sake of brevity, the linear design methodology is illustrated for the case of a single operating condition.

7.1. Linear controller design

At each trimming condition the linear feedback controllers were required to meet the following design specifications:

Zero steady state error. Achieve zero steady state values for all error variables in response to the fictitious input commands $\delta\tilde{\mathbf{p}}$ and $\delta\tilde{\phi}$ in $\boldsymbol{\zeta}$.

Bandwidth requirements. The input–output command response bandwidth for all command channels should be on the order of 5 rad/s.

Closed loop damping. The closed loop eigenvalues should have a damping ratio of at least 0.7.

It was also required that the steady-state deflection of the bow planes be $\delta_{\mathrm{b}} = 0$ rad.

The methodology selected for linear control system design was $\mathcal{H}_\infty$ state feedback. This method rests on a firm theoretical basis and leads naturally to an interpretation of control design specifications in the frequency domain. Furthermore, it provides clear guidelines for the design of controllers so as to achieve robust performance in the presence of plant uncertainty.

The first step in the controller-design procedure is the development of a synthesis model that can serve as an interface between the designer and the $\mathcal{H}_\infty$ controller synthesis algorithm. Consider the feedback system shown in Figure 9, where $\mathcal{P}_L(\boldsymbol{\eta}_C)$ is obtained from the linearized model of the AUV and $\mathcal{K}(\boldsymbol{\eta}_C)$ is the controller to be designed. The correspondence between the standard $\mathcal{H}_\infty$ controller design notation of Figure 9 and that introduced in Section 4 for incremental variables will be clear from the context. The block $\mathcal{J}(\boldsymbol{\eta}_C)$ within the dashed line is the synthesis model, which is derived from the linearized model of the plant by appending the

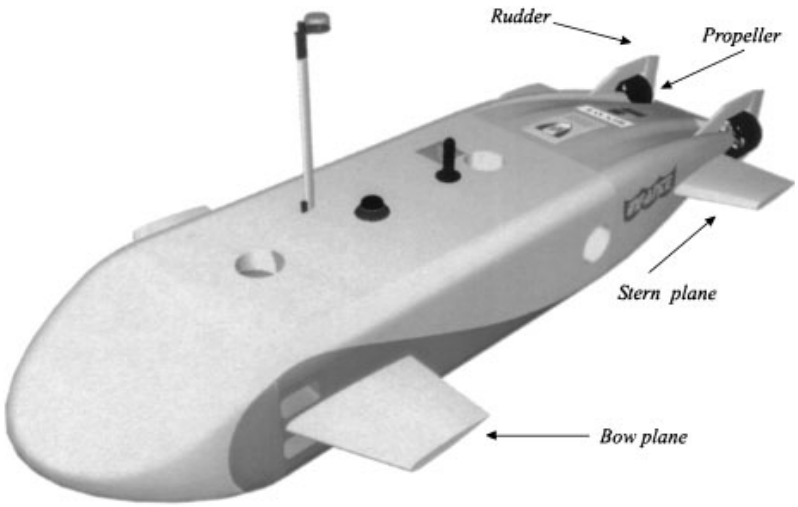

Figure 8. The Infante AUV.

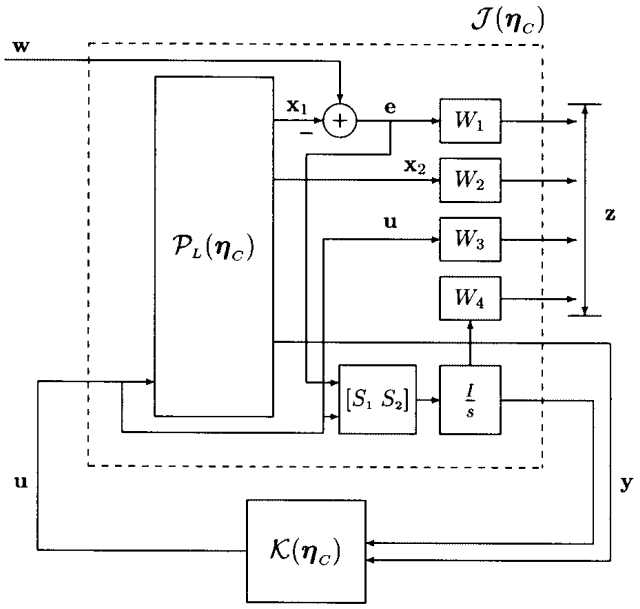

Figure 9. Synthesis model.

depicted weights. In practice, the weights serve as tuning 'knobs' which the designer can adjust to meet the desired performance specifications.

The signal **w** corresponds to the fictitious input vector ζ of Figure 5 and includes the input commands that must be tracked. The signal **u** corresponds to the control inputs to the system. The signal $\mathbf{x}_1$ contains the kinematic variables and includes the components of the state vector that must track the input commands. Finally, $\mathbf{x}_2$ consists of the remaining dynamic state variables. The blocks S_1 and S_2 select the kinematic tracking errors and the actuator signals

respectively, that must be driven to zero at steady state (along trimming trajectories). This justifies why the outputs of S_1 and S_2 drive a bank of integrators.

In the figure, W_1, W_2, W_3, and W_4 are non-dynamic weights that are used for controller tuning. Their outputs constitute the vector $\mathbf{z}$ that is reduced in the design process. The signal

$$y = \left[\mathbf{x}_{\text{dyn}}^{\text{T}}, \mathbf{x}_{\text{kin}_E}^{\text{T}}, \frac{\mathbf{p}_E^{\text{T}}}{s}, \frac{\phi}{s}, \frac{\delta_{\text{b}}}{s}\right]^{\text{T}}$$

consists of all the states of plant $\mathcal{P}_L(\boldsymbol{\eta}_C)$, together with the outputs of the appended integrators. The integrator gains in W_4 were adjusted to get the desired command response bandwidths and actuator decay ratio.

Given a design model, suppose that the feedback system is well posed and let $\mathcal{T}_{\mathbf{zw}}$ denote the closed loop transfer matrix from $\mathbf{w}$ to $\mathbf{z}$. Given γ positive, the $\mathcal{H}_\infty$ synthesis problem consists of finding, among all the controllers that yield a stable closed loop system, a sub-optimal controller $\mathcal{K}(\boldsymbol{\eta}_C)$ that makes the maximum energy amplification of the closed loop operator $\mathcal{T}_{\mathbf{zw}}$, denoted $\|\mathcal{T}_{\mathbf{zw}}\|_\infty$, less than γ. In this setting, γ plays the role of a design parameter. This problem was converted to an optimization problem and solved using the linear matrix inequalities technique presented in Reference [20].

A set of 6 linear controllers were computed for $\mathbf{V}_{\tau_c} = 2$ m/s, $\gamma_C \in \{0.0, 19.5\}$ deg, and $\dot{\psi}_C \in \{-4.6, 0.0, 4.6\}$ deg/s, with matrices $W_{(.)}$ and $S_{(.)}$ of the form

$$W_1 = 0.01 I_{6\times 6} \qquad W_2 = \begin{bmatrix} 10^{-2} I_{4\times 4} & 0 & 0 \\ 0 & 15 & 0 \\ 0 & 0 & 20 \end{bmatrix}$$

$$W_3 = \begin{bmatrix} 2 & 0 & 0 & 0 & 0 \\ 0 & 1 & 0 & 0 & 0 \\ 0 & 0 & 2 & 0 & 0 \\ 0 & 0 & 0 & 5 & 0 \\ 0 & 0 & 0 & 0 & 0.02 \end{bmatrix} \qquad W_4 = 10 I_{5\times 5}$$

$$S_1 = \begin{bmatrix} I_{3\times 3} & 0_{3\times 1} & 0_{3\times 2} \\ 0_{1\times 3} & 1 & 0_{1\times 2} \\ 0_{1\times 3} & 0 & 0_{1\times 2} \end{bmatrix} \qquad S_2 = \begin{bmatrix} 0_{4\times 1} & 0_{4\times 1} & 0_{4\times 3} \\ 0 & 1 & 0_{1\times 3} \end{bmatrix} \qquad \frac{I}{s} = \begin{bmatrix} \frac{1}{s} & 0 & 0 & 0 & 0 \\ 0 & \frac{1}{s} & 0 & 0 & 0 \\ 0 & 0 & \frac{1}{s} & 0 & 0 \\ 0 & 0 & 0 & \frac{1}{s} & 0 \\ 0 & 0 & 0 & 0 & \frac{1}{s} \end{bmatrix}$$

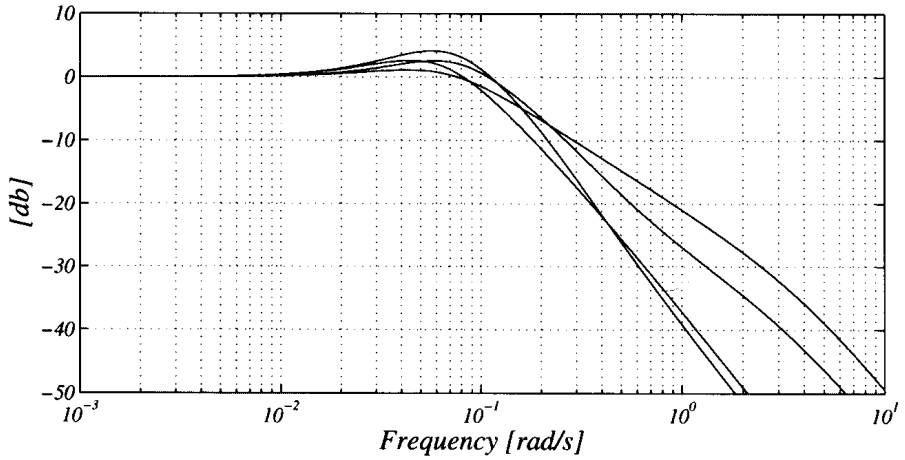

Figure 10. Frequency response for channels $\delta\tilde{\mathbf{p}}$ and $\delta\tilde{\phi}$.

for all controllers. For the case where $\gamma_C = 0.0$ deg and $\dot{\psi}_C = 0.0$ deg/s this design led to the set of closed loop eigenvalues

$$\begin{array}{lll} -0.08 & -0.33 \pm 0.33j & -22.69 \\ -0.29 \pm 0.29j & -0.65 \pm 0.03j & -24.73 \\ -0.30 \pm 0.25j & -1.11 \pm 0.22j & \\ -0.32 \pm 0.21j & -1.36 \pm 0.42j & \end{array}$$

that meet the closed loop system performance requirements. Figure 10 shows the Bode diagrams for the closed loop transfer functions from the fictitious linear position command inputs $\delta\tilde{\mathbf{p}}$ and $\delta\tilde{\phi}$ to $\delta\mathbf{p}$ and $\delta\phi$. The diagram shows that the performance requirements are met by the resultant closed loop system.

7.2. *Non-linear controller implementation*

A set of 6 controllers was computed for the combination of values of $\mathbf{V}_\tau$, $\dot{\psi}$, and γ presented above and their parameters interpolated according to the scheduling vector $\boldsymbol{\eta}$ in the given bounded domain.

The resulting non-linear gain scheduled controller was implemented using the trajectory tracking controller implementation methodology described in Section 5.

The gain scheduled controller implementation is depicted in Figure 6, where $\mathcal{K}(\boldsymbol{\eta})$ is easily obtained from the interpolation of the linear controllers derived in Section 7. In the case under study, the non-linear implementation strategy implies that *the only external commands to the trajectory tracking controller are* $\mathbf{p}_C$ *and* $\boldsymbol{\lambda}_C$, where the entries of $\boldsymbol{\lambda}_C$ are simply 0, 0, and $\int \dot{\psi}_C$. The first entry captures the fact that the value of roll throughout the trajectory should be kept at zero. The second entry is not relevant because the value of pitch at trimming is not imposed explicitly and therefore pitch error is not selected by matrix. Finally, notice that $\mathbf{p}_C$ and $\int \dot{\psi}_C$ are directly available from the reference trajectory generator.

It is important to stress that the controller implementation method presented above requires differentiation of some of the variables. In practice, the differentiation operator may simply be replaced by a causal system with transfer function

$$\frac{s}{\tau s + 1}$$

or by a simple finite difference operator for discrete-time implementation [10].

8. INTEGRATED GUIDANCE AND CONTROL SIMULATION

The performance of the integrated guidance and control system was evaluated in simulation with a non-linear model of the vehicle along a reference trajectory composed of the 7 segments of trimming trajectories presented in Table I. The reference for linear position in the x–y plane is an $\mathcal{S}$-shaped trajectory consisting of three straight lines 80 m long each and two semi-circumferences with radii of 48 m. The reference trajectory in the vertical plane transitions smoothly from a lower to a higher plateau with a slope of -10 deg. Notice that the vertical co-ordinate is positive down. In order to simplify the interpretation of the simulation results, the trajectory was generated with constant velocity $\mathbf{V}_{\tau_c} = 2.0$ m/s.

The desired and observed trajectories as well as the corresponding linear position errors are depicted in Figures 11–13. The controller activity and the vehicle model state variables are condensed in Figures 14–16 and 17–19, respectively. At the beginning of the manoeuvre, the actuation variables are essentially constant during the first 40 s. Upon entering the circular path, the rudder deflects to create a torque that will impart the desired rotational speed to the vehicle. Once the desired speed is reached, the rudder deflects slightly in the opposite direction to stabilize the rotation. This manoeuvre is characteristic of vehicles that are unstable in yaw.

At the middle of the first turn, the vehicle shows a pronounced rotation in pitch and converges rapidly to a pitch angle of 19.5 deg in order to track the desired flight path angle. This rotation is achieved by deflecting the common bow surfaces δ_b and the common stern surfaces δ_s in opposite directions, so as to generate a pure torque. When the vehicle reaches the desired orientation, δ_b and δ_s decrease. However, their values do not tend to zero, since they must counteract the restoring torque due to the combined effects of buoyancy and gravity.

When the vehicle reaches the end of the first turn, there is a strong deflection δ_r of the rudder to drive the velocity of rotation to zero. Similar comments apply to the remaining part of the trajectory.

Table I. Trimming values for the simulated trajectory

Time (s)	$\mathbf{V}_{\tau_c}$ (m/s)	ψ_C (deg/s)	γ_C (deg)
0–40	2.0	0.0	0.0
40–60	2.0	4.6	0.0
60–80	2.0	4.6	19.5
80–120	2.0	0.0	19.5
120–140	2.0	−4.6	19.5
140–160	2.0	−4.6	0.0
160–200	2.0	0.0	0.0

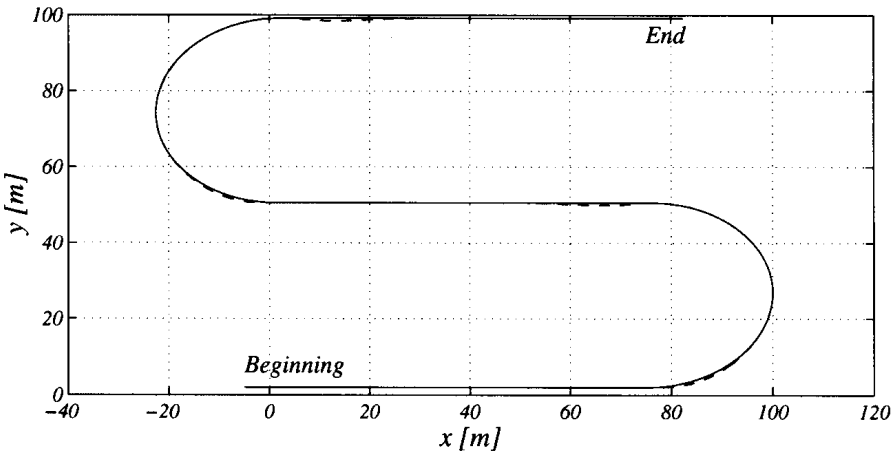

Figure 11. Reference and observed trajectory—horizontal plane.

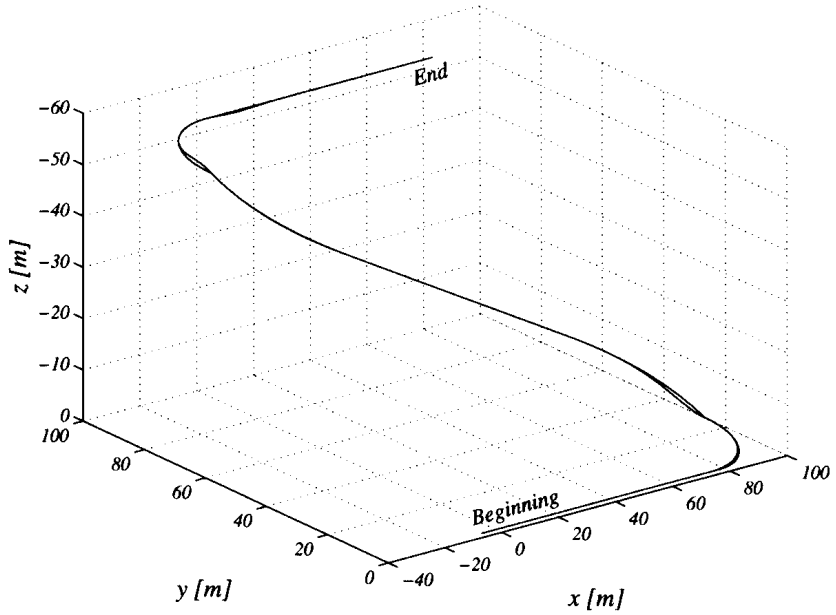

Figure 12. Reference and observed trajectory—three-dimensional view.

It is important to remark that thrust activity rises during manoeuvres that require large deflection of the control surfaces. This is required to counteract the increase in drag, which tends to slow down the vehicle.

9. CONCLUDING REMARKS

The paper presented a new methodology for the design of trajectory tracking controllers for autonomous vehicles. The new design method builds on three key results: (i) the trimming

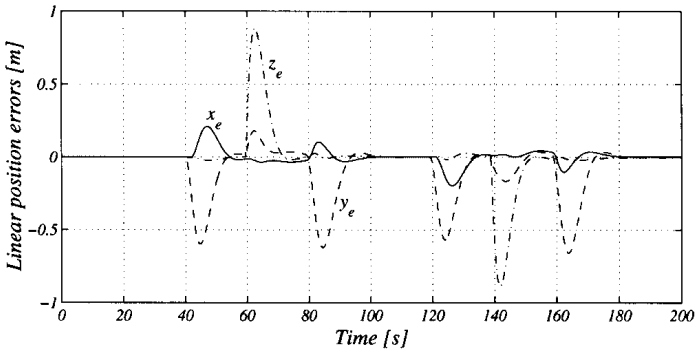

Figure 13. Linear position errors along the trajectory.

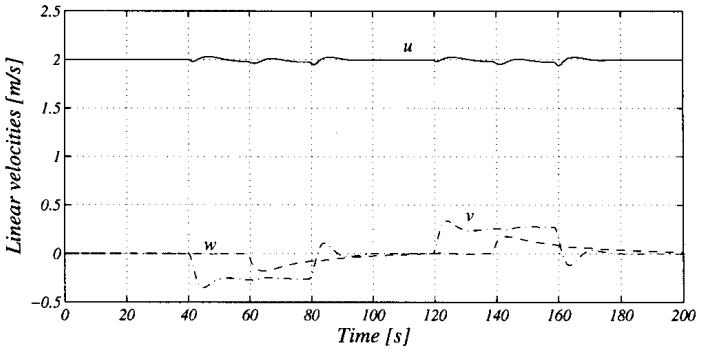

Figure 14. AUV state variables: linear velocities.

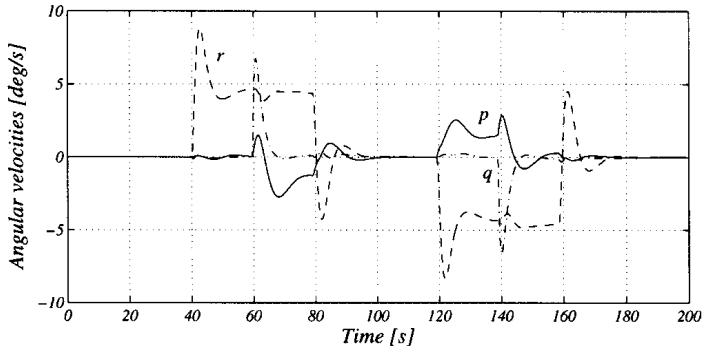

Figure 15. AUV state variables: angular velocities.

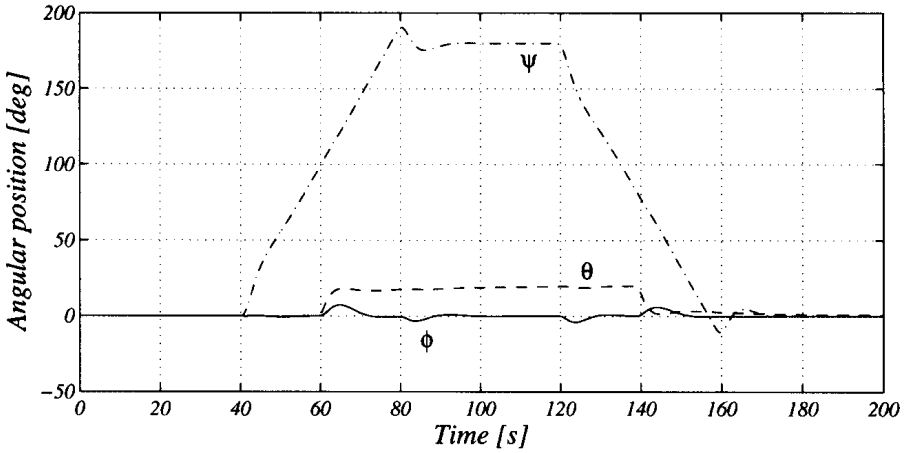

Figure 16. AUV state variables: angles of roll pitch and yaw.

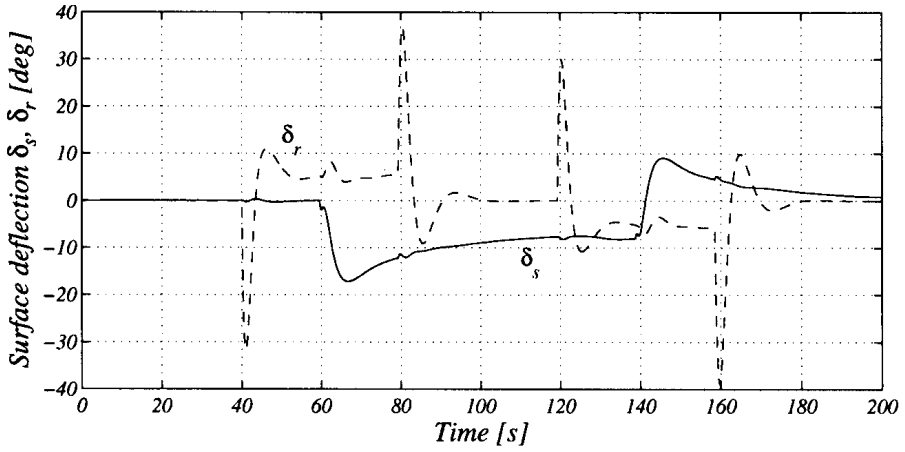

Figure 17. Control activity: rudder (δ_r), stern surfaces (δ_s).

trajectories of autonomous vehicles are helices parameterized by the vehicles linear speed, yaw rate, and flight path angle (trimming vector); (ii) tracking of a trimming trajectory by the vehicle is equivalent to driving a generalized tracking error to zero, and (iii) the linearization of the generalized error dynamics about any trimming trajectory is time-invariant. Based on these results, the problem of trajectory tracking system design was cast and solved in the framework of gain scheduling control theory.

A key feature of the controllers developed is their ability to automatically generate the trimming values for the plant inputs and for all state variables that are not required to track kinematic reference inputs. The new methodology is simple to apply and leads to a non-linear controller with a structure similar to that of the original linear designs. The paper described the application of the methodology developed to the design of a trajectory tracking controller for a

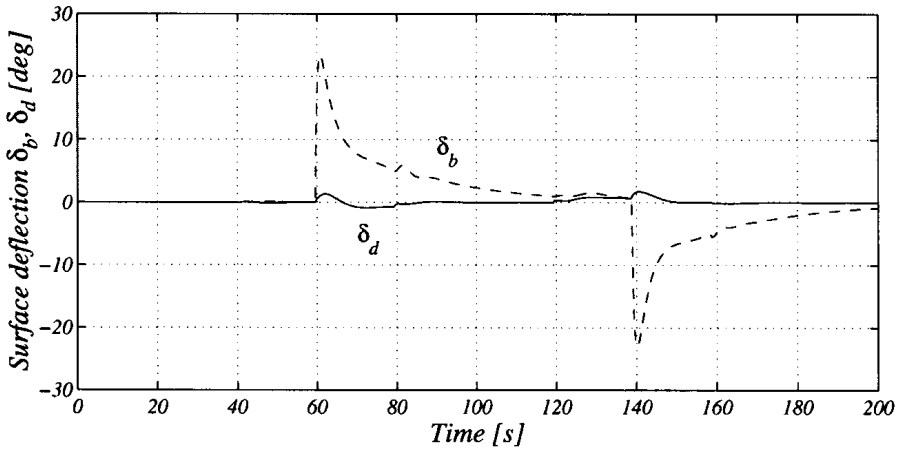

Figure 18. Control activity: differential (δ_d), bow surfaces (δ_b).

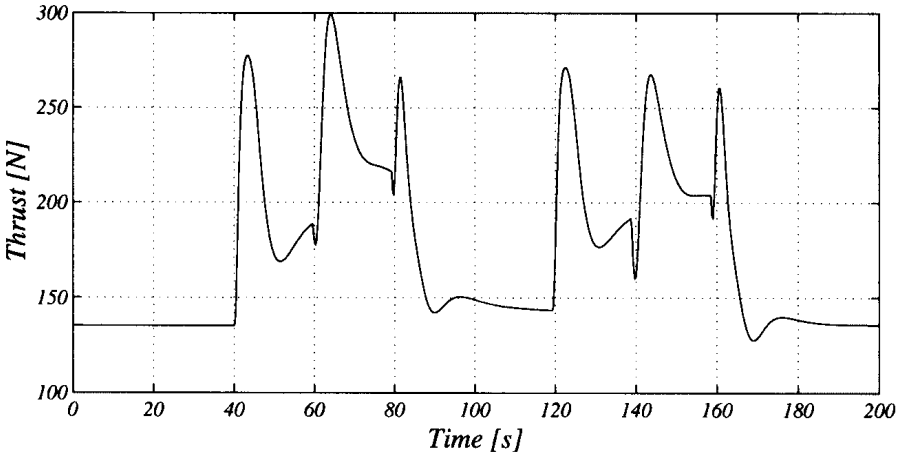

Figure 19. Control activity: thrust.

prototype autonomous underwater vehicle (AUV). The effectiveness of the new control laws was assessed in simulation. The results obtained show that the methodology derived holds considerable promise for practical applications. Future work will address the problem of vehicle trajectory tracking in the presence of external disturbances (currents and waves).

ACKNOWLEDGEMENTS

The work of C. Silvestre and A. Pascoal was partially supported by the Portuguese PRAXIS XXI Programme of FCT under projects INFANTE and MAROV and by MAST Programme of the EC under contract MAS3-CT97-0092 (ASIMOV). The work of I. Kaminer was supported by the Office of Naval Research under contract No. N0001497AF00002.

APPENDIX

This section presents some matrix and vector properties that are used in this paper. See Section 3.1 for the definition of vectors $\boldsymbol{\lambda}$ and $\boldsymbol{\omega}$ and matrices $\mathcal{R}$ and $\mathcal{Q}$. Given $\mathbf{u} = [u_x, u_y, u_z]^{\mathrm{T}}$ and $\mathbf{v} \in \mathbb{R}^3$, $\mathcal{S}(\mathbf{u})$ denotes the skew-symmetric matrix defined by

$$\mathcal{S}(\mathbf{u}) := \begin{bmatrix} 0 & -u_z & u_y \\ u_z & 0 & -u_x \\ -u_y & u_x & 0 \end{bmatrix} \tag{A1}$$

such that the cross product vector $\mathbf{u} \times \mathbf{v}$ equals $\mathcal{S}(\mathbf{u})\mathbf{v}$. In condensed form, $\mathcal{S}(\mathbf{u}) = \mathbf{ux}$. Recall that [21]

$$\mathcal{S}(\mathbf{u})\mathbf{v} = -\mathcal{S}(\mathbf{v})\mathbf{u} \tag{A2}$$

for any vectors $\mathbf{u}$ and $\mathbf{v}$ of compatible dimensions and that

$$\frac{\mathrm{d}}{\mathrm{d}t}\mathcal{R}(\boldsymbol{\lambda}) = \mathcal{R}(\boldsymbol{\lambda})\mathcal{S}(\boldsymbol{\omega}) \tag{A3}$$

Identity 10.1

Let $\mathbf{u}$ be a vector in $\mathbb{R}^3$. Then,

$$\frac{\mathrm{d}}{\mathrm{d}\boldsymbol{\lambda}}(\mathcal{R}\mathbf{u}) = -\mathcal{R}\mathcal{S}(\mathbf{u})\mathcal{Q}^{-1} \tag{A4}$$

and

$$\frac{\mathrm{d}}{\mathrm{d}\boldsymbol{\lambda}}(\mathcal{R}^{-1}\mathbf{u}) = \mathcal{S}(\mathcal{R}^{-1}\mathbf{u})\mathcal{Q}^{-1} \tag{A5}$$

Proof

To derive the first equality compute

$$\begin{aligned} \frac{\mathrm{d}}{\mathrm{d}t}(\mathcal{R}\mathbf{u}) &= \frac{\mathrm{d}}{\mathrm{d}t}(\mathcal{R})\mathbf{u} + \mathcal{R}\frac{\mathrm{d}}{\mathrm{d}t}\mathbf{u} \\ &= \mathcal{R}\mathcal{S}(\boldsymbol{\omega})\mathbf{u} + \mathcal{R}\frac{\mathrm{d}}{\mathrm{d}t}\mathbf{u} \\ &= -\mathcal{R}\mathcal{S}(\mathbf{u})\boldsymbol{\omega} + \mathcal{R}\frac{\mathrm{d}}{\mathrm{d}t}\mathbf{u} \end{aligned} \tag{A6}$$

Alternatively, using the chain rule

$$\begin{aligned} \frac{\mathrm{d}}{\mathrm{d}t}(\mathcal{R}\mathbf{u}) &= \frac{\mathrm{d}}{\mathrm{d}\boldsymbol{\lambda}}(\mathcal{R}\mathbf{u})\frac{\mathrm{d}}{\mathrm{d}t}\boldsymbol{\lambda} + \mathcal{R}\frac{\mathrm{d}}{\mathrm{d}t}\mathbf{u} \\ &= \frac{\mathrm{d}}{\mathrm{d}\boldsymbol{\lambda}}(\mathcal{R}\mathbf{u})\,\mathcal{Q}\boldsymbol{\omega} + \mathcal{R}\frac{\mathrm{d}}{\mathrm{d}t}\mathbf{u} \end{aligned} \tag{A7}$$

Equation (A4) follows by comparing Equations (A6) and (A7). To obtain Equation (A5), consider

$$\frac{\mathrm{d}}{\mathrm{d}t}(\mathcal{R}^{-1}\mathcal{R}) = \frac{\mathrm{d}}{\mathrm{d}t}(\mathcal{R}^{-1})\mathcal{R} + \mathcal{R}^{-1}\frac{\mathrm{d}}{\mathrm{d}t}(\mathcal{R}) = 0 \tag{A8}$$

where the equality $\mathcal{R}^{-1}\mathcal{R} = I, \ \forall \boldsymbol{\lambda}$ was used. Thus,

$$\begin{aligned}\frac{\mathrm{d}}{\mathrm{d}t}(\mathcal{R}^{-1}) &= -\mathcal{R}^{-1}\frac{\mathrm{d}}{\mathrm{d}t}(\mathcal{R})\mathcal{R}^{-1} \\ &= -\mathcal{S}(\boldsymbol{\omega})\mathcal{R}^{-1}\end{aligned}$$

As in the derivative of (A6), compute

$$\begin{aligned}\frac{\mathrm{d}}{\mathrm{d}t}(\mathcal{R}^{-1}\mathbf{u}) &= -\mathcal{S}(\boldsymbol{\omega})\mathcal{R}^{-1}\mathbf{u} + \mathcal{R}^{-1}\frac{\mathrm{d}}{\mathrm{d}t}\mathbf{u} \\ &= \mathcal{S}(\mathcal{R}^{-1}\mathbf{u})\boldsymbol{\omega} + \mathcal{R}^{-1}\frac{\mathrm{d}}{\mathrm{d}t}\mathbf{u}\end{aligned} \tag{A9}$$

Now, use the chain rule to obtain

$$\begin{aligned}\frac{\mathrm{d}}{\mathrm{d}t}(\mathcal{R}^{-1}\mathbf{u}) &= \frac{\mathrm{d}}{\mathrm{d}\boldsymbol{\lambda}}(\mathcal{R}^{-1}\mathbf{u})\frac{\mathrm{d}}{\mathrm{d}t}\boldsymbol{\lambda} + \mathcal{R}^{-1}\frac{\mathrm{d}}{\mathrm{d}t}\mathbf{u} \\ &= \frac{\mathrm{d}}{\mathrm{d}\boldsymbol{\lambda}}(\mathcal{R}^{-1}\mathbf{u})\,\mathcal{Q}\boldsymbol{\omega} + \mathcal{R}^{-1}\frac{\mathrm{d}}{\mathrm{d}t}\mathbf{u}\end{aligned} \tag{A10}$$

The second result follows readily from Equations (A9) and (A10).

REFERENCES

1. Pascoal A, Oliveira P, Silvestre C, Bjerrum A, Pignon J-P, Ayela G, Bruun S, Petzelt C. MARIUS: an autonomous underwater vehicle for coastal oceanography. *IEEE Robotics and Automation Magazine*, December 1997; 46–59.
2. Costello D, Kaminer I, Carder K, Howard R. The use of unmanned vehicle systems for coastal ocean surveys: scenarios for joint underwater and air vehicle missions. In *Proceedings of the Workshop on Undersea Robotics and Intelligent Control*, Lisbon, Portugal, March 1995.
3. Pascoal A, Paulo O, Silvestre C, Sebastião L, Rufino M, *et al.* Robotic ocean vehicles for marine science applications: the European ASIMOV project. In *OCEANS-2000*, Providence, RI, U.S.A., September 2000.
4. Healey A, Lienard D. Multivariable sliding mode control for autonomous diving and steering of unmanned underwater vehicles. *IEEE Journal of Oceanic Engineering* 1993; **OE-18**(3):327–339.
5. Lin C. *Modern Navigation, Guidance, and Control Processing*. Prentice-Hall: New Jersey, 1991.
6. Stevens BL, Lewis FL. *Aircraft Control and Simulation*. John Wiley & Sons: New York, U.S.A., 1992.
7. Vukobratovic M, Stojic R. *Modern Aircraft Flight Control. Lecture Notes in Control and Information Sciences*, vol. 109. Springer-Verlag: New York, U.S.A., 1988.
8. Papoulias F. Stability considerations of guidance and control laws for autonomous underwater vehicles in the horizontal plane. In *Proceedings of the 7th International Symposium on Unmanned Untethered Vehicle Technology*, Durham, NH, U.S.A., September 1991.
9. Rugh WJ, Shamma JS. A survey of research on gain-scheduling. *Automatica*, September 2000; 261–268.
10. Kaminer I, Pascoal A, Khargonekar P, Coleman E. A velocity algorithm for the implementation of gain-scheduled controllers. *Automatica* 1995; **31**(8):1185–1191.
11. Kaminer I, Pascoal A, Hallberg E, Silvestre C. Trajectory tracking for autonomous vehicles: an integrated approach to guidance and control. *AIAA Journal of Guidance, Control and Dynamics* 1998; **21**(1):29–38.
12. Al-Hiddabi SA. Position Tracking and Path Following for Flight Vehicles Using Non-linear Control. *Ph.D. Thesis*, Department of Aeronautics and Astronautics, University of Michigan, U.S.A., 2000.
13. Elgersma MR. Control of Nonlinear Systems Using Partial Dynamic Inversion. *Ph.D. Thesis*, University of Minnesota, Minneapolis, MI, USA, 1988.
14. Silvestre C. Multi-Objective Optimization Theory with Applications to the Integrated Design of Controllers/Plants for Autonomous Vehicles. *Ph.D. Thesis*, Department of Electrical Engineering, Instituto Superior Técnico, Lisbon, Portugal, 2000.
15. Abkowitz M. Lectures on ship hydrodynamics—steering and manoeuverability. *Technical Report* Hy-5, Technical University of Denmark, Hydrodynamics Department, Lyngby, Denmark, May 1964.
16. Craig JJ. *Introduction to Robotics Mechanics and Control*. Addison-Wesley Publishing Company: New York, U.S.A., 1986.

17. Silvestre C, Pascoal A. Control of an AUV in the vertical and horizontal planes: system design and tests at sea. *Transactions of the Institute of Measurement and Control* 1997; **19**(3):126–138.
18. Rugh WJ. Analytical framework for gain scheduling. *IEEE Control Systems Magazine* 1991; **11**(1):74–84.
19. Hanus R, Kinnaert M, Henrotte J. Conditioning technique, a general anti-windup and bumpless transfer method. *Automatica* 1987; **23**:729–739.
20. Boyd S, El Ghaoui L, Feron E, Balakrishnan V. *Linear Matrix Inequalities in System and Control Theory*. Society for Industrial and Applied Mathematics (SIAM): Philadelphia, U.S.A., 1994.
21. Spong MW, Vidyasagar M. *Robot Dynamics and Control*. John Wiley & Sons: New York, U.S.A., 1989.

